Exploration of novel hexahydropyrrolo[1,2-e]imidazol-1-one derivatives as antiviral agents against ZIKV and USUV [*Chen R, *Francese R co-first authors]

Exploration of novel hexahydropyrrolo[1,2-e]imidazol-1-one derivatives as antiviral agents against ZIKV and USUV

Ran Chen [a,e,1], Rachele Francese [b,1], Na Wang [c], Feng Li [a], Xia Sun [a], Bin Xu [a], Jinsong Liu [c], Zhuyun Liu [d], Manuela Donalisio [b], David Lembo [b,*], Guo-Chun Zhou [a,e,*]

[a] School of Pharmaceutical Sciences, Nanjing Tech University, Nanjing 211816, Jiangsu, China

[b] Laboratory of Molecular Virology and Antiviral Research, Department of Clinical and Biological Sciences, University of Turin, S. Luigi Gonzaga Hospital, 10043 Orbassano, Turin, Italy.

[c] Guangzhou Institutes of Biomedicine and Health, Chinese Academy of Sciences, Guangzhou 510530, China

[d] School of Pharmacy, Taizhou Polytechnic College, Taizhou 225300, Jiangsu, China

[e] Xitaihu Lake Industrial College, Nanjing Tech University, Changzhou 213149, Jiangsu, China

[1] These authors contributed equally to this paper.

* Corresponding authors: gczhou@njtech.edu.cn (G.-C. Zhou) and david.lembo@unito.it (D. Lembo).

Abstract

Zika virus (ZIKV) and Usutu virus (USUV) are two emerging flaviviruses mostly transmitted by mosquitos. ZIKV is associated with microcephaly in newborns and the less-known USUV, with its reported neurotropism and its extensive spread in Europe, represents a growing concern for human health. There is still no approved vaccine or specific antiviral against ZIKV and USUV infections. The main goal of this study is to investigate the anti-ZIKV and anti-USUV activity *in vitro* of a new library of compounds and to preliminarily investigate the mechanism of action of the selected hit compounds *in vitro*. Two potent anti-ZIKV and anti-USUV agents, namely **ZDL-115** and **ZDL-116**, were discovered, both presenting low cytotoxicity, cell-line independent antiviral activity in the low micromolar range and ability of reducing viral progeny production. The analysis of the structure-activity relationship (SAR) revealed that introduction of 2-deoxyribose to 3-arene was fundamental to enhance the solubility and improve the antiviral action. Additionally, we demonstrated that **ZDL-115** and **ZDL-116** are significantly active against both viruses when added on cells for at least 24 h prior to viral inoculation or immediately post-infection. The docking analysis showed that **ZDL-116** could target host vitamin D receptor (VDR) and viral proteins. Future experiments will be focused on compound modification to discover analogues that are more potent and on the clarification of the mechanism of action and the specific drug target. The discovery and the development of a novel anti-flavivirus drug will have a significant impact in a context where there are no fully effective antiviral drugs or vaccines for most flaviviruses.

Key words: hexahydropyrrolo[1,2-e]imidazol-1-one; antiviral agents; Zika virus; Usutu virus; structure-activity relationship.

Graphic abstract

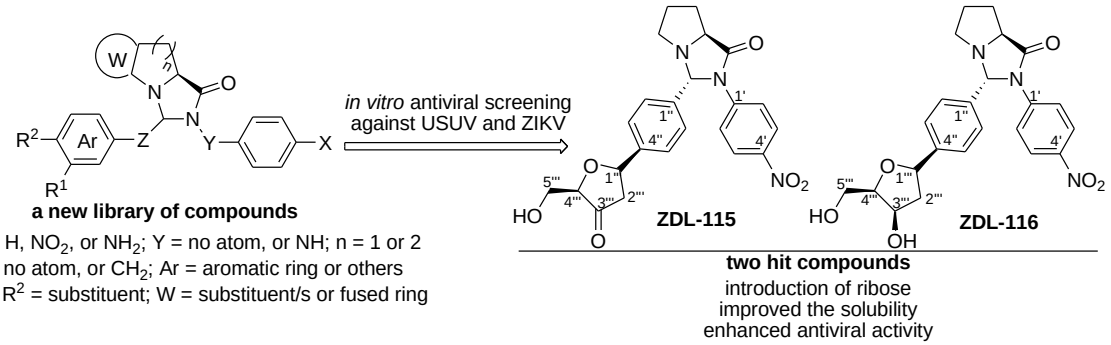

a new library of compounds

X = H, NO_2, or NH_2; Y = no atom, or NH; n = 1 or 2
Z = no atom, or CH_2; Ar = aromatic ring or others
R^1, R^2 = substituent; W = substituent/s or fused ring

two hit compounds

introduction of ribose
improved the solubility
enhanced antiviral activity

Highlights:

- Two hexahydropyrrolo[1,2-e]imidazol-1-one derivatives are anti-flavivirus agents
- Introduction of 2-deoxyribose to 3-arene improves the inhibition of ZIKV and USUV
- **ZDL-115** and **ZDL-116** are able to reduce the production of infectious viral progeny
- Data suggested that the compounds exert both preventive and therapeutic activity
- Docking analysis showed that VDR and viral proteins are the binders of **ZDL-116**

1. Introduction

Infectious diseases caused by new emerging or suddenly re-emerging pathogens are surging in recent years and are becoming a significant public health concern that requires global cooperation [1]. In particular, the (re)emergence of arthropod-borne viruses has been widely reported and mainly attributed to intensive growth of global transportation systems, arthropod adaptation to increasing urbanisation, limited mosquito population containment and land perturbation [2]. Among them, flaviviruses, such as Zika virus (ZIKV), Dengue virus (DENV), West Nile virus (WNV), Japanese encephalitis virus (JEV) and other less well-known viruses belonging to the same genus, can emerge unexpectedly in human populations and cause a spectrum of potentially severe diseases including hepatitis, vascular shock syndrome, encephalitis, acute flaccid paralysis, congenital abnormalities and fetal death [3,4]. Therefore, the continued development of countermeasures to treat or prevent human infections is urgent.

Briefly, ZIKV is mainly transmitted by *Aedes aegypti* mosquitos and has been associated with the Guillain-Barré syndrome in adults and with a variety of congenital defects, including microcephaly, in infants born to infected mothers. It was first discovered in Africa in 1950, but its potential effect on public health was not recognized until the virus caused outbreaks in the Pacific from 2007 to 2015 and began spreading throughout the Americas in 2015. The last major epidemic counted more than 500 000 confirmed ZIKV cases and around 3000 cases of zika virus congenital syndrome (CSZ), driving the World Health Organization to declare a public health emergency of international concern in 2016 [5]. To date, a total of 86 countries and territories have reported evidence of mosquito-transmitted Zika infection. Although transmission of ZIKV has declined in the Americas, the virus still poses a public health threat, as shown by recent outbreaks reported in India, Southeast Asia and Africa [6]. At present, we do not have tools to predict where and when the next epidemic will happen, but the large numbers of susceptible persons residing in *Aedes*-infested regions makes a re-emergence of ZIKV likely. The less-known Usutu virus (USUV), which was firstly reported in Central African Republic in 1981 [7], is drawing increasing attention of the scientific community due to its extensive spread in Europe [9,10]. It is closely related to JEV and WNV, sharing with the latter a similar enzootic cycle and the major vector, i.e. the *Culex pipiens* mosquito [9]. A large retrospective study, conducted on over 900 patients suggested that USUV human infections may have been largely underestimated, probably because numerous USUV infections are asymptomatic, and indicated a seroprevalence of 6.5% in the European population [10]. Clinical disease with moderate flu-like manifestations (rash, fever, and headache) may also

occur, but the neurotropism of USUV currently represents a growing concern for human health. In more than 32 human cases to date, indeed, severe neurological disorders, including facial paralysis, encephalitis, meningitis, and meningoencephalitis, in both immunocompromised and immunocompetent patients have been observed. However, the full clinical presentation of USUV infection still needs to be better defined [11-13].

Regarding the structural characteristics, ZIKV and USUV are enveloped viruses with a single-stranded RNA of positive polarity. Their genome encodes for a single polyprotein that, after cleavage, generates 3 structural proteins (capsid C, premembrane and envelope) and 7 non-structural (NS) proteins — NS1 (involved in RNA replication and particle assembly), NS2A (RNA replication and immune evasion), NS2B (cofactor of NS3), NS3 (major viral protease), NS4A (cofactor of NS3), NS4B (RNA replication and immune evasion) and NS5 (RNA synthesis and modification) — which are essential for viral replication. All the above-mentioned proteins, along with some host factors essential for viral replication, can potentially be antiviral drug targets [14,15]. Nevertheless, there is still no approved vaccine or specific antiviral for ZIKV and USUV and the clinical treatment consists in a supportive care [5,9]. With the aim of responding to this unmet medical need, some repurposing drugs were investigated as anti-ZIKV molecules [16,17] and many new compounds were reported to have inhibitory effects against ZIKV replication and infection [18-24]. The hexahydropyrrolo[1,2-e]imidazol-1-one (the fused bicyclic ring of pyrrolidine and 4-imidazolidinone), tetrahydroimidazo[1,5-a]quinolin-3(3aH)-one (the fused tricyclic ring of indoline and 4-imidazolidinone) and tetrahydroimidazo[1,5-a]indol-1-one (the fused tricyclic ring of tetrahydroquinoline and 4-imidazolidinone) were discovered as active scaffolds against DENV, ZIKV, or/and JEV infections in our previous study [25-29]. In this study, a new library of compounds based on the abovementioned active scaffolds was tested against ZIKV and USUV infections *in vitro*. We reported the design, synthesis and identification of two significantly active compounds mounted on 2-deoxyribose moiety, namely **ZDL-115** and **ZDL-116**, endowed with anti-ZIKV and anti-USUV activity and with low cytotoxicity. Additionally, their structure-activity relationship (SAR) and their preliminary mechanism of action were investigated.

2. Results and discussion

2.1. Design

In our previous study (**Chart 1**), compound **ZD-7**, one of the hexahydropyrrolo[1,2-e]imidazol-1-one derivatives [25,26] was demonstrated to be active against DENV2 infection *in vitro*, with EC_{50} values of 39.4 μM [25]. Subsequently, the functionalized derivatives resulted to have improved EC_{50} values less than 12 μM against the same virus. In particular, the compound **ZD-6** resulted to be able to significantly inhibit the production of DENV1, 3, 5, JEV and ZIKV at 10 μM [27]. In that study, we demonstrated that the scaffold of hexahydropyrrolo[1,2-e]imidazol-1-one derivatives possesses VDR modulatory activity [26,27], which was potentially associated with its antiviral properties [27]. Further explorations found that some fused tricyclic derivatives (**Chart 1B**) of tetrahydroimidazo[1,5-a]quinolin-3(3aH)-one [28] and tetrahydroimidazo[1,5-a]indol-1-one [29] are also active against ZIKV and DENV infections *in vitro*. In this study, with the aim of discovering more potent antiviral agents with reasonable pharmacological property, we designed and screened a new library of compounds (**Chart 1B**) based on the bicyclic or tricyclic derivatives of 4-imidazolidinone fused with pyrrolidine, or quinoline and indoline against ZIKV and USUV. We identified two hit compounds from the library, **ZDL-115** and **ZDL-116**, as the most active anti-ZIKV and anti-USUV agents (see sections 2.4 and 2.5). The design of **ZDL-115** and **ZDL-116** is based on two considerations: 1) the introduction of a ribose moiety as part of the further functionalization of arene (**Chart. 1**) may enhance the solubility of the molecule and improve the pharmaceutical characteristics; 2) 2-deoxyribose arene could mimic a nucleoside [30-32] so that **ZDL-115** and **ZDL-116** (**Chart 1**) can possibly act as inhibitors of viral protein/s associated with nucleoside and nucleotide [18]. In order to establish the SAR of **ZDL-115** and **ZDL-116** for rational drug discovery, we also designed a series of analogues of **ZDL-115** and **ZDL-116**.

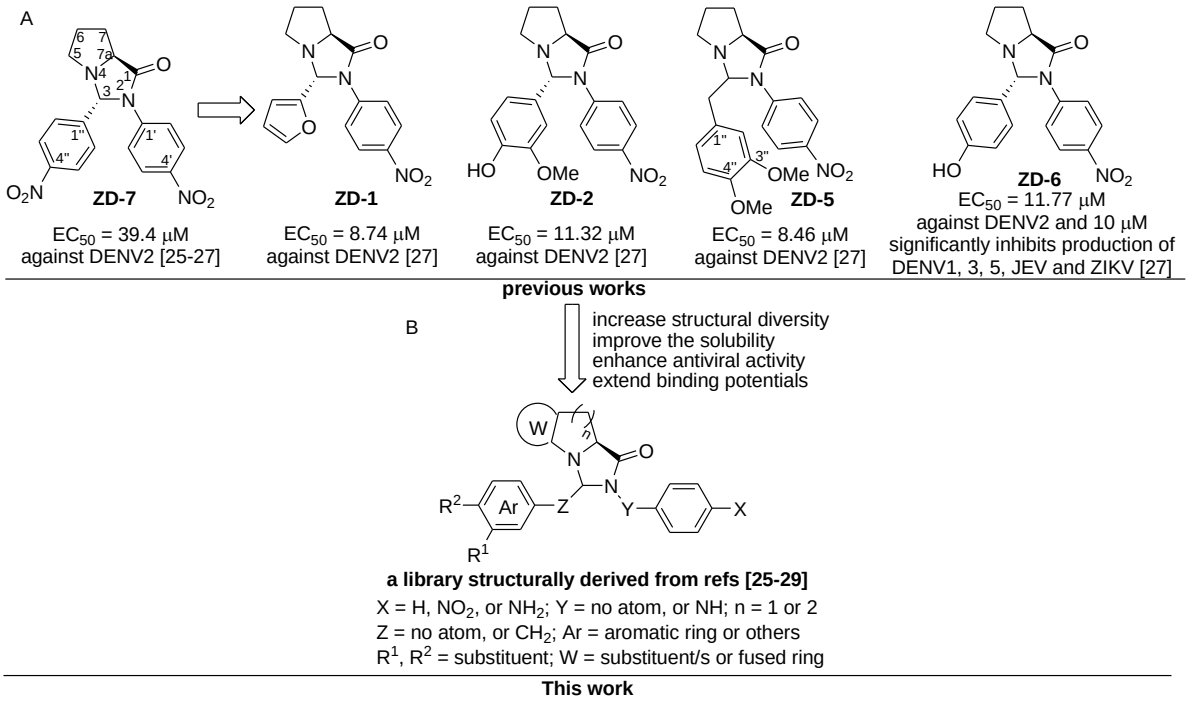

Chart 1. The previous reported DENV or/and ZIKV inhibitors based on hexahydropyrrolo[1,2-e]imidazol-1-one scaffold [27] (A), a new library designed on the basis of our previous reports [25-29] for this work (B).

2.2. Synthesis of titled compounds

All of these tested compounds from **Chart 1** and **Schemes 1-3** are listed in **Table S1** (Supplementary material). The synthesis of two hit compounds, **ZDL-115** and **ZDL-116**, is shown in **Scheme 1**. The starting material of **1** was prepared according to the references [32,33]. Then, Heck coupling of **1** with *p*-iodobenzenealdehyde (**2**) was conducted by the catalysis of tris(dibenzylideneacetone)dipalladium ($Pd_2(dba)_3$) and tris(*o*-methylphenyl)phosphine ($(o\text{-tolyl})_3P$) in triethylamine (TEA) and 1,4-Dioxane at 80 °C to afford the key intermediate aldehyde **3** (55 % yield) specifically in β form, properly due to bulkiness of 4'-OTBDPS as previously suggested in a similar reaction condition [34-38]. Adopted from our previous work [25,26], condensation of *N*-Boc proline (**4**) with *p*-nitroaniline (**5**) followed by de-protection of Boc group by acidic condition provided intermediate amide **6**. The reaction of aldehyde **3** with amide **6** was fulfilled in the presence of TEA to form *N*,*N*'-acetal **7**. Finally, desilylation of **7** by tetrabutylammonium fluoride (TBAF) afforded ketone of **ZDL-115**, and then reduction at 0 °C of ketone of **ZDL-115** by $NaBH_4$ to deliver hydride from less steric hindered α face gave 4'''β-OH isomer of **ZDL-116** as a dominant product, which is different from reported 4'''α-OH

reduced by $NaBH(OAc)_3$ [34-38] as OAc of $NaBH(OAc)_3$ can exchange with 5'''-CH_2OH and provides opportunity for intramolecular reduction to deliver [H] from β-face [34-38].

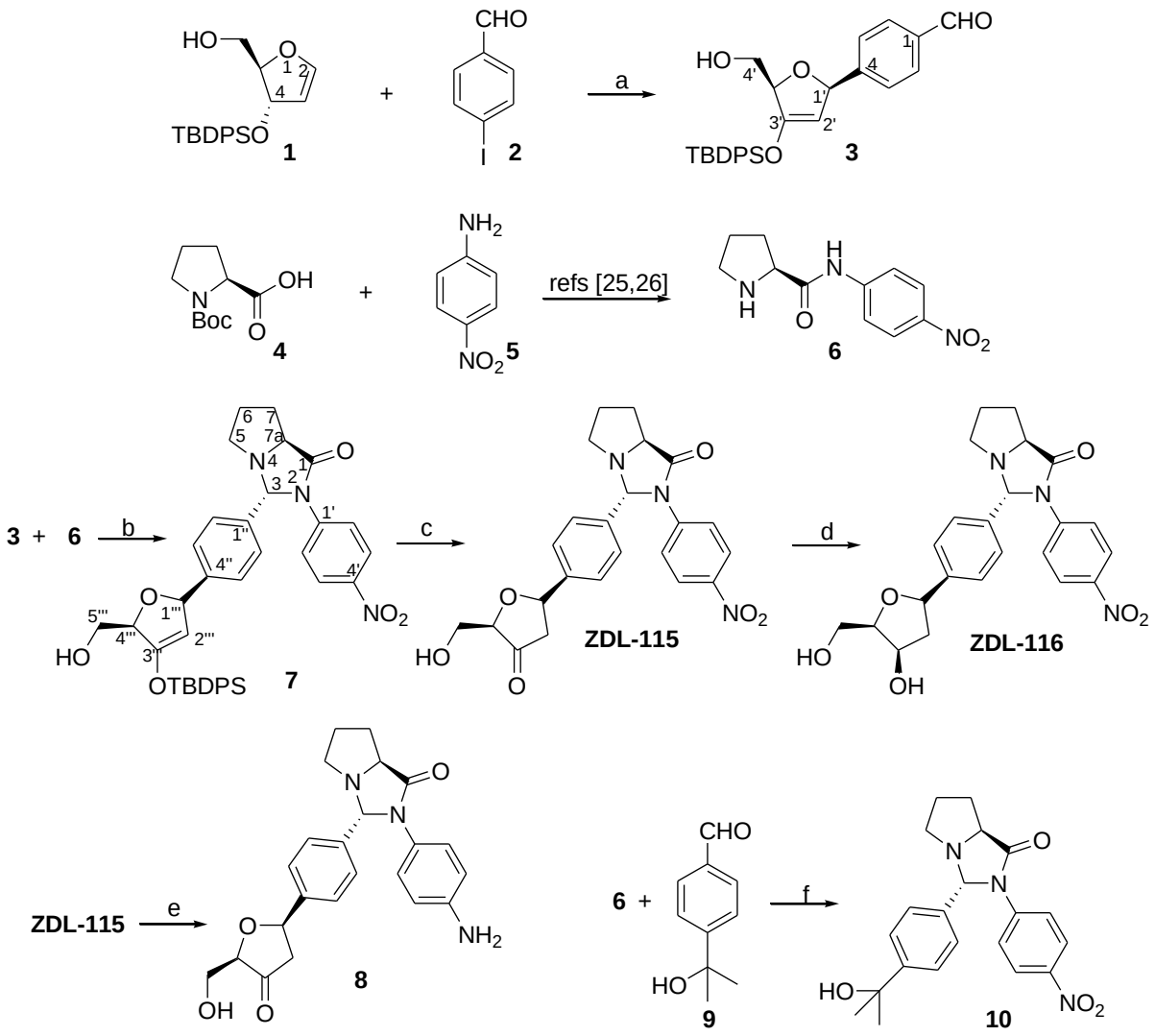

Scheme 1. Reagents and condition: (a) $Pd_2(dba)_3$, (*o*-tolyl)$_3$P, TEA, 1,4-Dioxane, 80 °C, 6 h, 55%; (b) TEA, Toluene, 110 °C, 4 h, 74%; (c) TBAF, THF, 0 °C to rt, 1 h, 76%; (d) $NaBH_4$, THF, 0 °C, 1 h, 50%; (e) Pd/C, H_2, THF, rt, 3 h, 54%; (f) TEA, acetonitrile, 70 °C, 2 h, 69%.

The absolute configuration of **ZDL-116** was determined by ^{1}H NMR and ^{1}H-^{1}H NOESY in DMSO-d_6 (**Fig. 1** and **Figs. S1a-S1o**). Comparison of ^{1}H NMR spectra of **ZDL-116** in DMSO-d_6 and in DMSO-d_6-treated D_2O, two peaks of 4.77 and 4.46 ppm are 5'''-O*H* and 3'''-O*H*. There are very strong NOEs between two O-*H*s themselves, indicating two O-*H*s in *cis* form, while two O-*H*s exhibit NOEs with 7.36 ppm of 1'''β-aromatic 3''-*H*, which strongly

correlates with 1'''α-*H* (4.69 ppm), confirmed that the 3'''-O*H* is 3'''β-O*H*. Meanwhile, 3.56 and 3.685 ppm of 5'''-CH_2 exhibit very weak NOE with 1'''β-aromatic 3'''-*H* (7.36 ppm). Furthermore, 1'''α-*H* (4.69 ppm) has a NOE correction with 4.29 ppm, which has very strong NOE with 3'''β-O*H* (4.77), thus, the signal of 4.29 ppm is 3'''α-*H*. 1'''α-*H* (4.69 ppm) has strong NOE with its two adjacent hydrogen of 2'''-H_2 at 1.60 and 2.54 ppm, while the signal of 1.60 ppm but not of 2.54 ppm establishes strong NOE correlation with 3'''β-O*H* (4.77 ppm) and 1'''β-aromatic 3''-*H* (7.36 ppm), demonstrating 1.60 and 2.54 ppm are 2'''β-*H* and 2'''α-*H* signals, respectively. 2'''α-*H* (2.54 ppm) has strong NOE correlation with signals of 3'''α-*H* (4.29) and 4'''α-*H* (3.68 ppm), supporting that signals of 3.68, 4.29, 2.54 and 4.69 ppm are *cis* configuration. Altogether, the configuration and conformation of **ZDL-116** is the same as the structure depicted in **Fig. 1**.

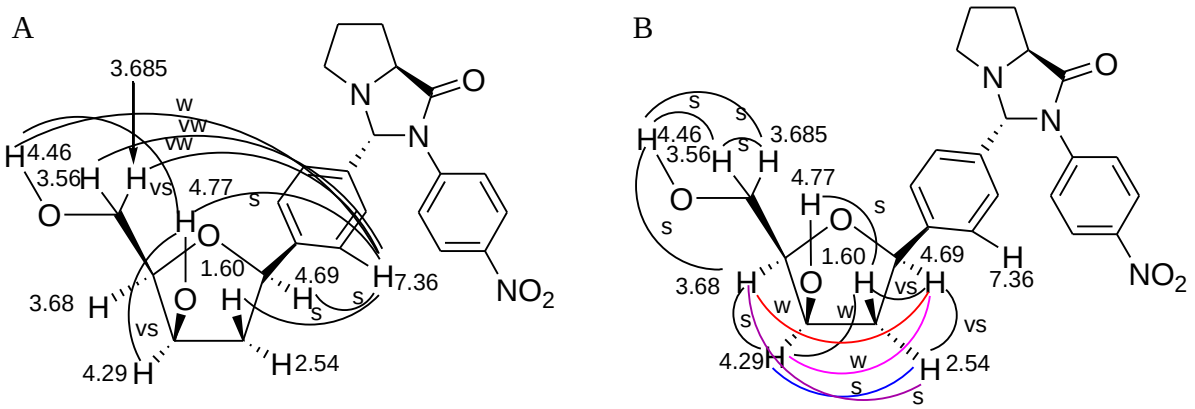

Fig. 1. NOE determination of absolute configuration of **ZDL-116** in DMSO-d_6. (A) NOE correlation starting from 1'''β-aromatic 3''-*H* (7.36 ppm). (B) NOE correlation starting from 1'''α-*H* (4.69 ppm). (Note: It is difficult to discern overlapped peaks of 3.68 and 3.685 ppm, belonging to 4'''α-*H* and one of two 5'''-*H*s, and their NOEs.)

In order to study preliminary SAR, compounds modified at N2-, C4'- and C4'-positions were prepared as shown in **Scheme 1**, **Scheme 2** and **Scheme 3**. Firstly, hydrogenation with H_2 balloon of nitro group of **ZDL-115** into amine by the catalysis of Pd/C in tetrahydrofuran (THF) provided amine compound **8** (**Scheme 1**), which will be compared with **ZDL-115** for their anti-ZIKV and anti-USUV activities to explore the importance of 4'-nitro group. 2'-Hydroxyethyl compound **10**, mimicking 2-deoxyribose of **ZDL-115** and **ZDL-116**, was prepared by the reaction of **6** with *p*-(2-hydroxypropan-2-yl)benzaldehyde (**9**) (**Scheme 1**).

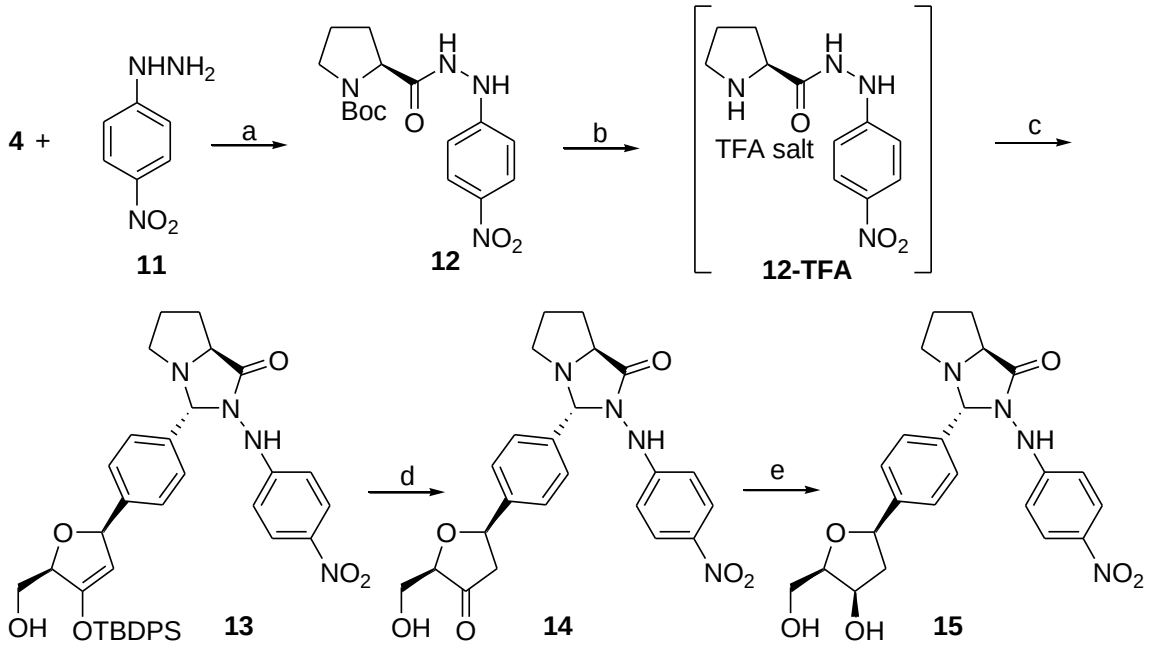

Scheme 2. Reagents and condition: (a) 1-Methylimidazole, MsCl, DCM, 0 °C to rt, 6 h, 80%; (b) TFA, DCM, rt, 2 h, 90%; (c) **3**, Toluene, TEA, 110 °C, 6 h, 65%; (d) TBAF, THF, 0 °C to rt, 1 h, 75%; (e) $NaBH_4$, THF; 0 °C, 1 h, 50%.

In **Scheme 2**, condensation of *N*-Boc proline **4** and 4-nitrophenyl hydrazine (**11**) produced acylhydrazine **12**, which then was treated with trifluoroacetic acid (TFA) to form TFA salt of **12-TFA**, followed by the reaction of TFA salt with **3** gave hydrazine product **13**, which is a counterpart of **7**. After desilylation of **13** by TBAF to give the ketone **14** and reduction by $NaBH_4$ to afford the diol **15**. Acylhydrazine analogues of **14** and **15** are parallel to corresponding amides of **ZDL-115** and **ZDL-116**; therefore, they will be used to reveal the structural tolerance of anti-ZIKV and anti-USUV by the elongation of amine products (**ZDL-115** and **ZDL-116**) into hydrazine products (**14** and **15**).

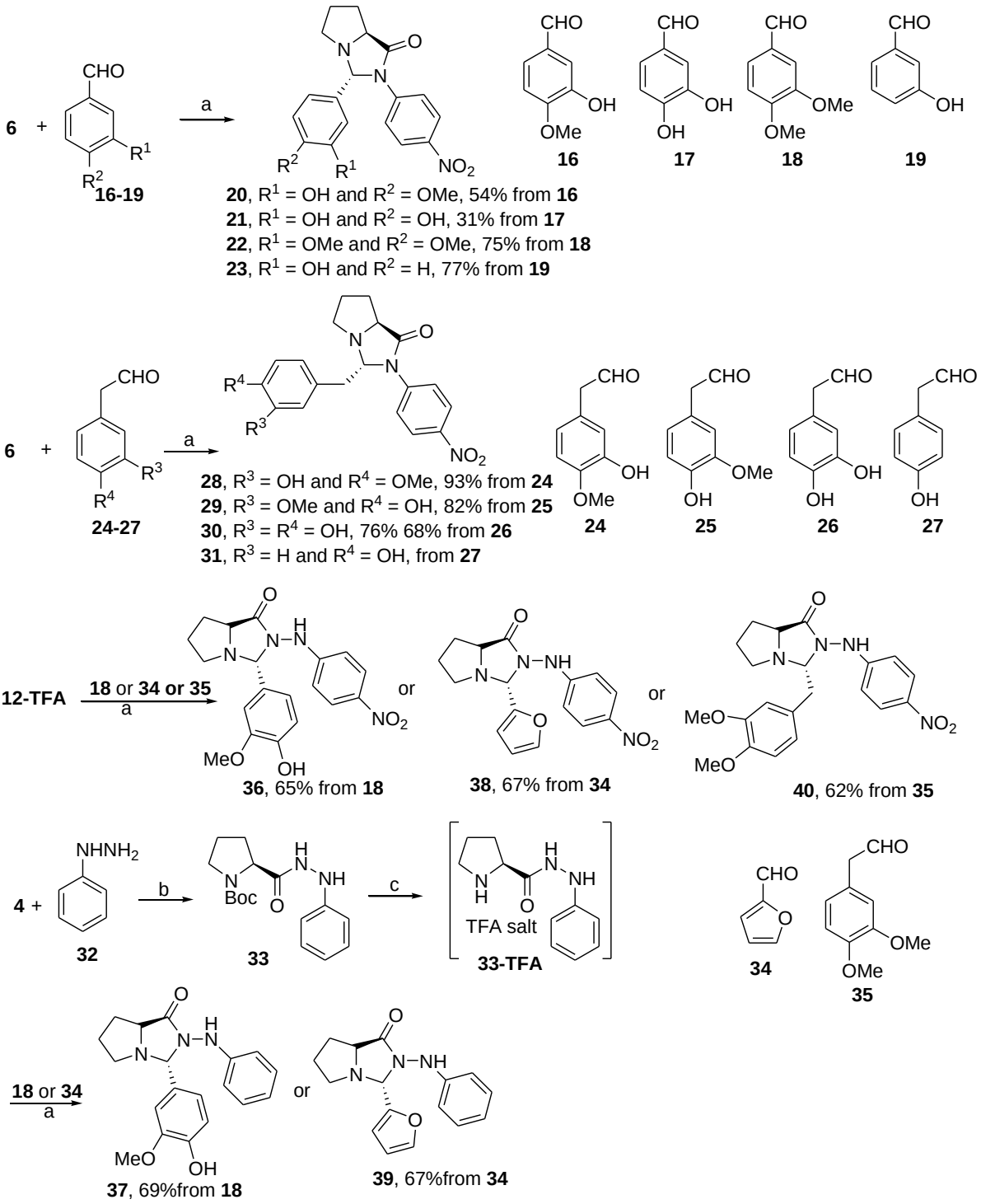

Scheme 3. Reagents and condition: (a) TEA, acetonitrile, 70 °C, 2 h; (b) DCM, DMAP, DCC, 0 °C to rt, overnight, 83%; (c) TFA, DCM, rt, 2 h.

In order to increase the structural diversity, different substituents at 3-arene were introduced by the reaction of aromatic aldehydes of **16**-**19** or aromatic acetaldehydes of **24**-**27** with amide **6** to afford corresponding **20**-**23** or **28**-**31**, respectively, of the fused bicyclic derivatives of pyrrolidine and 4-imidazolidinone (**Scheme 3**). In addition, annulation of

aldehydes of **18**, **34** and **35** with acyl phenylhydrazine (**12**) and acyl 4-nitrophenylhydrazine (**33**) yielded compounds of **36-40** as expanding structures of **14** and **15** (**Scheme 3**).

2.3. Solubility comparison of ZDL-115 and ZDL-116 with the previously reported compound ZD-2

With **ZDL-115** and **ZDL-116** in hand, we tested and compared their solubility in *i*-propanol, DMSO and 1.38% DMSO aqueous solution in deionized water with those of the previously reported active compound **ZD-2** [27] (**Chart 1A**). As shown in **Table 1**, **ZDL-115** and **ZDL-116** have better solubility in these solvents than **ZD-2** as expected, showing that introduction of 2-deoxyribose increases their hydrophilicity. Interestingly, **ZDL-115**, compared to **ZDL-116**, seems better soluble in *i*-propanol and DMSO; on the contrary, no significant solubility difference was observed in aqueous solution.

Table 1. Solubility of the titled compounds

compound	Solubility (mg/mL) at 25 °C		
	i-propanol	DMSO	1.38% DMSO aqueous solution in deionized water
ZD-2	1.17	37.5	0.518
ZDL-115	8.57	130	≥ 0.897
ZDL-116	7.32	96	≥ 0.947

2.4. Antiviral screening of a library of hexahydropyrrolo[1,2-e]imidazol-1-one, tetrahydroimidazo[1,5-a]quinolin-3(3aH)-one and tetrahydroimidazo[1,5-a]indol-1-one derivatives and identification of two hit compounds

The first set of antiviral experiments was addressed to investigate the anti-ZIKV and anti-USUV activity of a library of 116 new bicyclic or tricyclic derivatives of 4-imidazolidinone fused-pyrrolidine, -tetrahydroquinoline or -indoline, which were designed on the basis of our published scaffolds [25-29]. The general structure is shown in **Chart 1B** and **Table S2**. Three concentrations of each compound (100, 33, 11 μM) were initially tested by means of the focus reduction assay described in the "**Experimental**" section. Briefly, a fixed amount of ZIKV or USUV (MOI = 0.02) was pre-treated with three serial concentrations (100 μM, 33 μM and 11 μM) of the tested compound for 1 h at 37 °C. These mixtures (virus with dilutions of the compound) were then added to pre-seeded Vero cells for the necessary time for viral replication

(20 h or 30 h). The ZIKV or USUV-infected cells were detected by indirect immunostaining and the % of viral infection was calculated by comparing the treated with the untreated wells. Compounds showing low solubility, i.e. showing the presence of precipitates on the treated cell monolayer, or showing microscopically visible cytotoxicity in at least one of the tested concentrations were excluded for further studies. Two compounds resulted active against both viruses at 100 µM (**ZDL-44** and **ZSD-24**) and only one compound completely inhibited ZIKV infection at 100 µM and 33 µM (**ZSD-30A**). Among the tested compounds, only **ZDL-115** and **ZDL-116** showed 100% inhibition of both ZIKV and USUV infectivity at all the tested concentrations. Additionally, no morphological alteration of the **ZDL-115-** or **ZDL-116-**treated cell monolayers was detectable comparable to the untreated controls. Considering these preliminary results, **ZDL-115** and **ZDL-116** were selected for the prosecution of the study. In the pie chart represented in **Fig. 2**, the result summary from this first step of screening is presented and complete results are reported in **Table S2**.

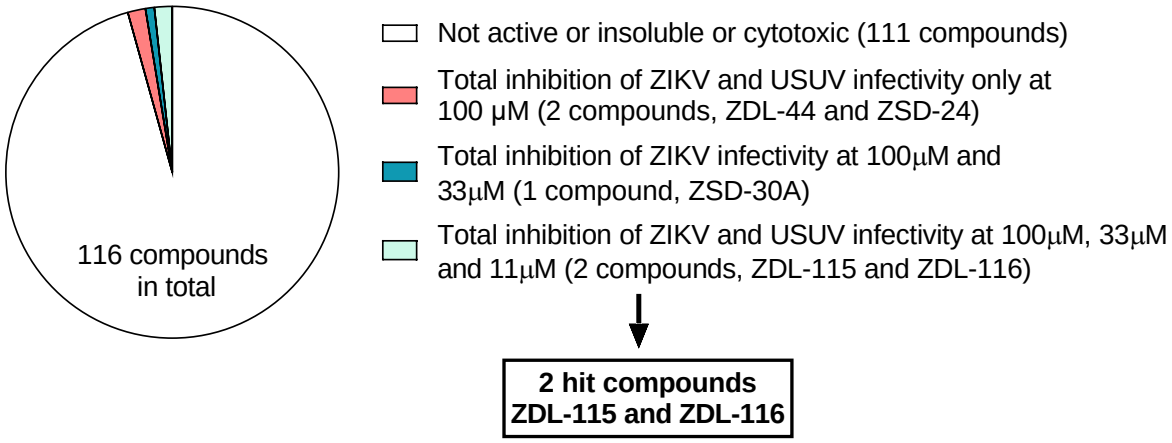

Fig. 2. Summary of the results obtained from the library screening against ZIKV and USUV. 116 New fused bicyclic or tricyclic derivatives bearing scaffolds of hexahydropyrrolo[1,2-e]imidazol-1-one [25-27], tetrahydroimidazo[1,5-a]quinolin-3(3aH)-one [28] and tetrahydroimidazo[1,5-a]indol-1-one [29] were tested against ZIKV and USUV infections by means of virus inhibition assay. The pie chart summarize the screening results that are extensively reported in **Table S2**. The majority of compounds resulted toxic in at least one of the tested doses (white). Two compounds resulted active against both viruses at 100µM (light red) and only one compound completely inhibited ZIKV infection at 100 µM and 33 µM (blue). Among the tested compounds, **ZDL-115** and **ZDL-116** were identified as the hit compounds, showing complete inhibition of ZIKV and USUV infectivity at 100 µM, 33 µM and 11 µM (light blue).

2.5. Validation of the antiviral activity of ZDL-115 and ZDL-116 against ZIKV and USUV

After having identified **ZDL-115** and **ZDL-116** as hit compounds, we further investigated their antiviral action. We performed the virus inhibition assay generating dose-response curves on three different cell-lines, i.e. Vero, A549 and Huh7 cells, which are well-reported models for the *in vitro* study of ZIKV and USUV infectivity [39,40] (dose-response curves are graphically reported in **Fig. S2**). As shown in **Fig. S2** and **Table 2**, both compounds are endowed with significant and cell line-independent anti-ZIKV and anti-USUV activity, with 50% effective concentration (EC_{50}) values in the low micromolar range, from 2.26 μM to 9.73 μM, for all the tested experimental conditions. No significant difference was observed in the antiviral activities of **ZDL-115** and **ZDL-116**, suggesting that the small difference in their chemical structures did not alter their antiviral potential. Subsequently, in order to exclude the possibility that the observed antiviral action was due to a cytotoxic effect of the compounds, viability and cytotoxicity assays (MTS and LDH assays, respectively) were performed by treating cells under the same experimental conditions as the virus inhibition assay described above. Results indicated that **ZDL-115** and **ZDL-116** were not toxic for cells, showing 50% cytotoxic concentration (CC_{50}) values > 500μM and favourable selectivity indexes (CC_{50}/EC_{50} > 50) for all tested conditions. Since no approved anti-ZIKV and anti-USUV compound is currently available, we tested chloroquine as the reference compound, a known endocytosis inhibitor previously reported to be active against ZIKV *in vitro* [41-45]. As flaviviruses generally enter cells by clathrin-mediated endocytosis, we tested chloroquine also as a positive compound against USUV *in vitro* [46]. Results are reported in **Table 2**.

Moreover, we demonstrated that the anti-ZIKV activity of the compounds was not strain restricted. Indeed, comparable EC_{50} values were obtained testing **ZDL-115** and **ZDL-116** against ZIKV HPF2013, a strain belonging to the Asian lineage, differently to the previously tested MR766, that belongs to the African one (**Table S3**) [47]. The ability of the compounds to inhibit ZIKV infection was also confirmed by means of plaque reduction assays. Results reported in **Table S4**, showed a significant ability of **ZDL-115** and **ZDL-116** of reducing ZIKV plaque formation, thus suggesting that the compounds are active over multiple replicative cycles.

Table 2. Antiviral activity of **ZDL-115** and **ZDL-116** against ZIKV and USUV on different cell lines

Cell line	Compound	Virus	EC_{50} [a] (μM) (95% CI [e])	EC_{90} [b] (μM) (95% CI)	CC_{50} [c] (μM) (95% CI)	SI [d]
Vero	**ZDL-115**	USUV	2.76 (2.60 – 2.91)	4.34 (3.93 – 4.87)	> 500	> 181
		ZIKV [f]	9.73 (8.97 – 10.58)	15.43 (13.73 – 17.73)	> 500	> 51
	ZDL-116	USUV	2.53 (2.33 – 2.75)	3.89 (3.46 – 4.47)	> 500	> 198
		ZIKV	7.96 (7.31 – 8.65)	12.34 (9.79 – 14.66)	> 500	> 63
	Chloroquine	USUV	8.30 (5.90 – 11.67)	28.18 (14.08 – 56.43)	114.8 (83.95-157.0)	13.83
		ZIKV	1.53(1.12 – 2.10)	5.77 (2.97 – 11.21)	135.8 (103.0-179.0)	88.76
A549	**ZDL-115**	USUV	6.82 (4.97 – 9.37)	15.16 (8.92 – 25.77)	> 500	> 73
		ZIKV	3.80 (2.63 – 5.72)	10.22 (3.93 – 26.58)	> 500	> 132
	ZDL-116	USUV	6.42 (5.69 – 7.26)	12.00 (9.99 – 14.42)	> 500	> 78
		ZIKV	3.95 (2.07 – 6.17)	10.86 (3.36 – 35.04)	> 500	>127
	Chloroquine	USUV	4.24 (2.21-8.11)	60.12 (13.2-273.8)	144.2 (116.0-179.3)	34.00
		ZIKV	5.99 (3.10-11.58)	50.26 (11.67-216.4)	80.45 (59.95-108.0)	13.43
Huh7	**ZDL-115**	USUV	4.00 (3.73 – 4.28)	6.28 (4.02 – 9.81)	> 500	> 125
		ZIKV	2.36 (1.78 – 3.14)	4.19 (3.00 – 5.85)	> 500	> 212
	ZDL-116	USUV	3.91 (3.44 – 4.46)	5.77 (2.09 – 15.93)	> 500	> 128
		ZIKV	2.26 (2.07 – 2.47)	4.26 (3.77 – 4.82)	> 500	> 221
	Chloroquine	USUV	4.82 (3.92 – 5.93)	11.79 (7.19 – 19.35)	75.49 (58.8-96.92)	15.66

		ZIKV	0.95 (0.57 – 1.57)	2.36 (0.79 – 7.04)	58.51 (45.74-74.84)	61.59

[a] EC_{50}: half maximal effective concentration.

[b] EC_{90}: 90 % effective concentration.

[c] CC_{50}: half maximal cytotoxic concentration calculated by means of the MTS assay and confirmed through the LDH assay (data not shown); for the reference compound (chloroquine) the CC_{50} was evaluated by means of MTS assay.

[d] SI: selectivity index.

[e] CI: confidence interval.

[f] Data refer to the results obtained with ZIKV strain MR766; the results obtained with ZIKV HPF2013 are reported in **Table S3**.

Even though we have not yet established the link between antiviral activity of **ZDL-115** and **ZDL-116** with the VDR signal pathway, considering that the scaffold of **ZDL-115** and **ZDL-116** was previously reported to exhibit VDR modulatory activity [26,27], we compared the antiviral activity of these compounds with the one of **EB1089** (Seocalcitol), a commercial vitamin D analogue. As shown in **Table 3**, **EB1089** showed EC_{50} values comparable to **ZDL-115** and **ZDL-116**, but it was highly toxic on Vero cells, showing low CC_{50} values (very close to its EC_{90} values) and making it impossible to exclude a residual cytotoxicity at the effective doses. The cytotoxic effect may derive from **EB1089**'s partial VD structure and to its consequential VDR binding activity [48,49]. These data indicated that our compounds are more active and safer than **EB1089** bearing vitamin D scaffold and underline that the potential involvement of VDR activated pathways in the antiviral activity of our compounds remains to be clarified.

Table 3. Antiviral activity of **EB1089** against ZIKV and USUV

Cell line	Compound	Virus	EC_{50} [a] (µM) (95% CI [e])	EC_{90} [b] (µM) (95% CI)	CC_{50} [c] (µM) (95% CI)	SI [d]
Vero	**EB1089**	USUV	2.13 (1.17 – 3.88)	9.94 (2.47 – 39.96)	11.9	6
		ZIKV (MR766)	7.51 (4.96 – 11.37)	9.86 (3.65 – 26.58)	11.0	1.5
		ZIKV(HPF2013)	2.83 (0.32 – 25.3)	15.25 (2.36 – 98.51)	11.0	3.9

[a] EC_{50}: half maximal effective concentration.

[b] EC_{90}: 90 % effective concentration.

[c] CC_{50}: half maximal cytotoxic concentration calculated by means of the MTS assay; the CC_{50} value obtained through the LDH assay is 7.37 μM.

[d] SI: selectivity index.

[e] CI: confidence interval.

Next, we evaluated whether **ZDL-115** and **ZDL-116** are able to affect the production of infectious viral progeny. To test the ability of two compounds to inhibit multiple cycles of viral replication, we performed a virus yield reduction assay, treating cells during and post infection with 2 highly effective and not toxic concentrations, 5 μM or 15 μM, for 48 h and then performing titration of the harvested virus samples. As graphically reported in **Fig. 3**, both compounds significantly affected ZIKV and USUV progeny production, reaching a titer reduction of two orders of magnitude at 15 μM (raw data are reported in **Table S5**). As expected, no significant difference in the antiviral activity of **ZDL-115** and **ZDL-116** was observed.

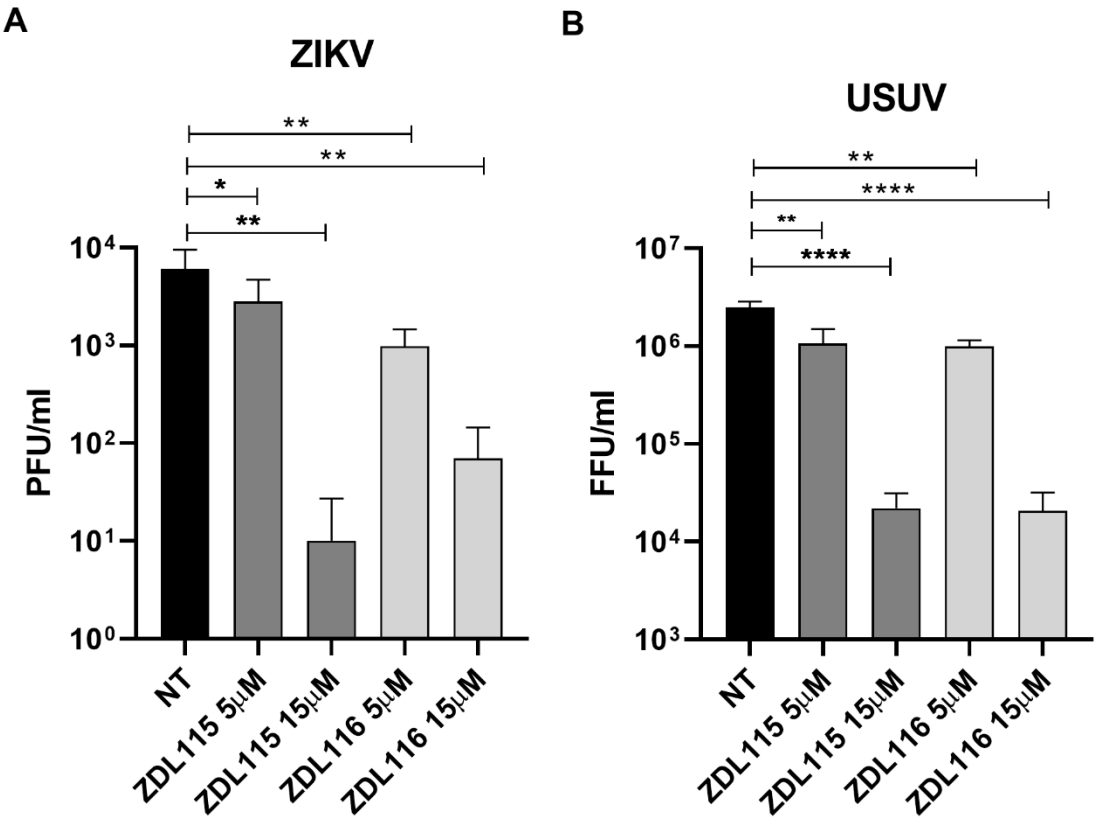

Fig. 3. ZDL-115 and **ZDL-116** reduce ZIKV and USUV progeny production. Vero cells were treated and infected with a mixture of the compound (5 μM or 15 μM) and ZIKV or USUV (MOI = 0.1) for 2 h at 37°C. The virus inoculum was then removed and cells were incubated with medium containing the compound (5

µM or 15 µM) for 48 h. Supernatants were clarified and cell-free virus infectivity titers were determined by the plaque assay (ZIKV) or focus reduction assay (USUV). The viral titers are expressed PFU/ml (ZIKV) or FFU/ml (USUV) and are shown as mean plus SEM for three independent experiments. Treated and control samples were compared with one-way ANOVA. (* = $p_{anova} < 0.01$, (** = $p_{anova} < 0.001$; **** = $p_{anova} < 0.00001$)

Our results are in line with previous studies [25-27] reporting the anti-flavivirus action of fused bicyclic derivatives of hexahydropyrrolo[1,2-e]imidazol-1-one. In particular, compounds of **Chart 1A** showed a significant antiviral activity against different strains of DENV, JEV and ZIKV [27]. Herein, our new compounds, more hydrophilicity and lipophilicity than the previous ones (**Table 1**), resulted strongly active against two ZIKV strains and against USUV, confirming that the scaffold is endowed with a potential broad spectrum anti-flavivirus action. Additionally, we observed an overall improvement of the SI values compared to the previously tested derivatives [25,27], suggesting that our hit compounds are endowed with more favourable characteristics for further development. To the best of our knowledge, this is the first study investigating the scaffold's antiviral activity against USUV, and our positive results indicate that this virus can now be added to the list of targeted viruses.

2.6. Antiviral screening of ZDL-115 and ZDL-116's analogues and SAR

After the identification of **ZDL-115** and **ZDL-116** as highly effective antiviral compounds, we designed and synthesized 17 analogues of **ZDL-115** and **ZDL-116** (**Scheme 2** and **Scheme 3**) in order to discover more active compounds and to understand the preliminary SAR against ZIKV and USUV infections. Firstly, the antiviral activity of the compounds presented in **Scheme 2** illustrates the importance of the basic scaffold. Amine **8** loses anti-ZIKV and anti-USUV activity after 4'-nitro of **ZDL-115** was reduced into 4'-amine. Compound **10** of mimicking 1'''-, 2'''- and 3'''- of 2-deoxyribose was not active against ZIKV and USUV. Moreover, 4'-nitrophenyl hydrazine analogues of **14** and **15** corresponding to **ZDL-115** and **ZDL-116**, respectively, were not ZIKV and USUV inhibitors. These results show that 4'-nitro group, 2-deoxyribose and *N*-2 directly attached arene (**Scheme 2**) favour for exhibiting anti-ZIKV and anti-USUV activity. Secondly, chemical diversity for drug discovery and SAR was explored (**Scheme 3**). Derivatives of 4-nitrophenylhydrazine and phenylhydrazine as expanding structures modified at C3-position by various aryl or arylmethyl with multiple substitutions showed no anti-ZIKV or anti-USUV activity comparable to **ZDL-115** and **ZDL-116** (**Fig. 4**); whereas, **37** and **39**, as acyl phenylhydrazine derivatives, only showed a partial inhibition (< 50%) of viral infectivity at 33 µM for both viruses. By comparing **37** and **39** with

corresponding **36** and **38** of acyl 4-nitrophenylhydrazine derivatives, we observed that 4'-H group is slightly superior to 4'-nitro group against ZIKV and USUV infections. Furthermore, we made comparison of these compounds with reported compounds **ZD-1**, **ZD-2**, **ZD-5** and **ZD-6**. Compound **40** as an acyl 4-nitrophenylhydrazine derivative was inactive against ZIKV and USUV, while compound **ZD-5** of 4-nitrophenylamide derivative is known to be a potent DENV2 inhibitor [27], also indicating that acyl 4-nitrophenylhydrazine is not a good group for the scaffold. Two substitutions at 3"- and 4"-positions of compound **20** (3"-OH-4"-OMe), compound **21** (3",4"-di-OH) and compound **22** (3",4"-di-OMe) do not confer antiviral activity against ZIKV and USUV infections, while compound **ZD-2** (**Chart 1**, 3"-OMe-4"-OH) is active against DENV2 infections [27]; in parallel, compound **23** (3'-OH) is not active against ZIKV and USUV, while compound **ZD-6** (**Chart 1**, 4'-OH) is active against DENV1-4, JEV and ZIKV [27], demonstrating that different occupied positions of two groups of OMe and OH affect antiviral activity. Similarly, compound **ZD-5** (**Chart 1**, 3",4"-di-OMe) was reported as a potent DENV2 inhibitor [27], but compounds **28** (3"-OH-4"-OMe), **29** (3"-OMe-4"-OH), **30** (3",4"-di-OH) and **31** (3"-H-4"-OH) were not ZIKV and USUV inhibitors. Moreover, two 3"-OMe-4"-OH derivatives of compound **36** derived from hydrazine and compound **ZD-2** (**Chart 1**) derived from amide exhibited different antiviral activity: the former was inactive against ZIKV and USUV, the latter was a potent inhibitor of DENV2 infection [27]; 2-furanyl analogue of **ZD-1** (**Chart 1**) is an antiviral agent but corresponding **38** was found to be inactive against ZIKV and USUV infection, suggesting that 4-nitrophenylhydrazine is not as good as 4-nitrophenylamine for the structural moiety. Altogether, these results allowed us to clarify the primary SAR (**Fig. 4**, **Tables S2** and **S6**) of our compounds and provide the rationale that optimal combination of C3 group, substituent/s at arene and its/their occupied position/s, amide or hydrazine, may be the important factor to construct potent ZIKV and USUV inhibitors.

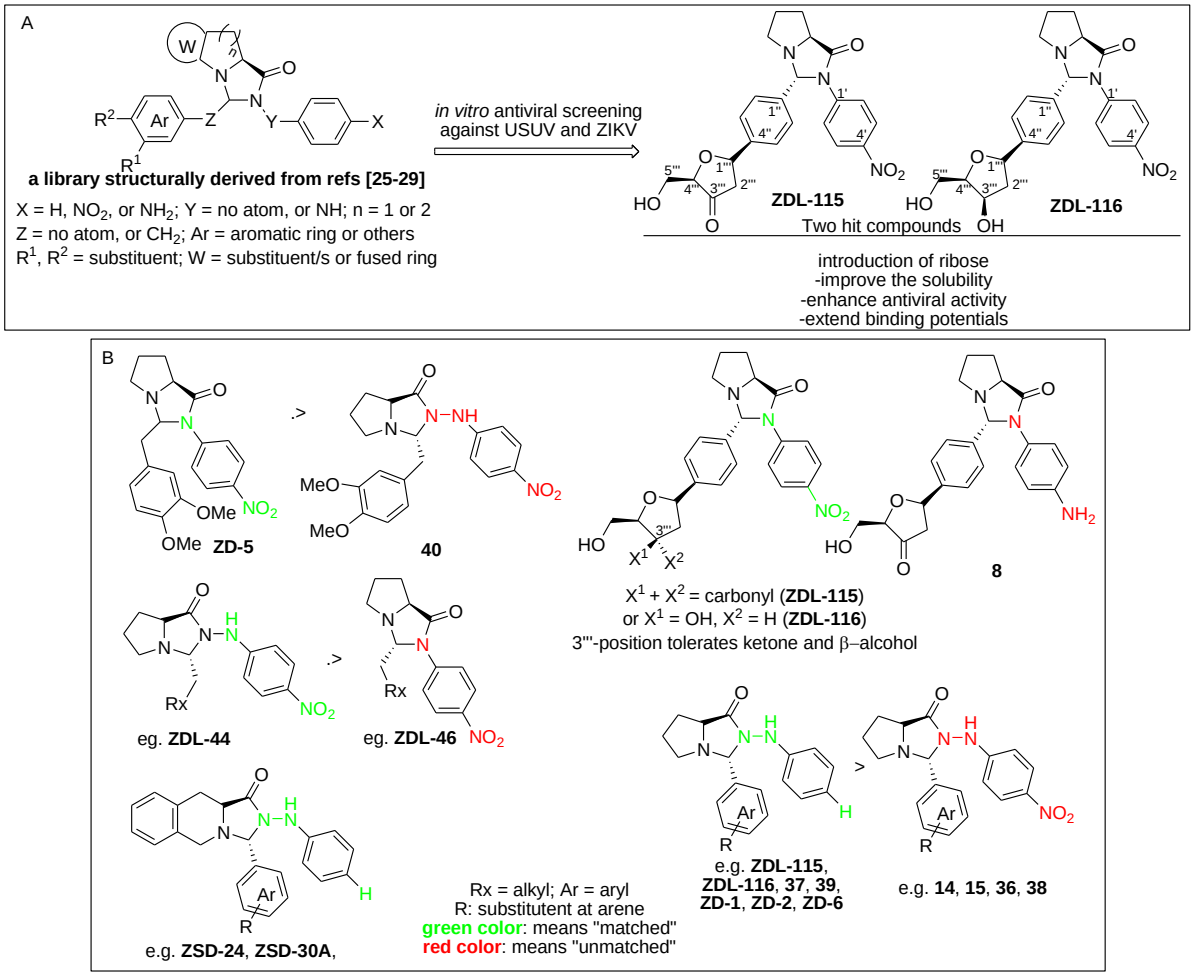

Fig. 4. (A) Summary of *in vitro* antiviral screening of the library and the two hit antiviral inhibitors, **ZDL-115** and **ZDL-116**, identified in this work; (B) Representative primary SAR, "matched" means the favourable combination and "unmatched" represents unfavourable combination.

2.7. Preliminary study of the mechanism of antiviral action of ZDL-115 and ZDL-116

The preliminary investigation of the mechanism of action of **ZDL-115** and **ZDL-116** was performed by means of the time of addition assays described in the "**Experimental**" section and results are shown in **Fig. 5** and in **Table S6** and **Table S7**. Briefly, cells were treated at different time points: 24 h before infection, 2 h before infection, during infection for 2 h or post infection in order to identify the specific phase of the viral replicative cycle inhibited by the compound. Overall, the results indicated that **ZDL-115** and **ZDL-116** exert their antiviral activity when added on cells for at least 24 h prior to the infection or immediately after viral entry into the host cell. No antiviral activity was observed adding the compounds 2 h before infection or during infection for 2 h. More specifically, in the case of ZIKV, both **ZDL-115**

and **ZDL-116** were significantly active when added on cells immediately after virus entry for 30 h. The long pre-treatment (24 h before infection) also showed a significant antiviral action, but presenting EC_{50} values 5-fold higher than post-treatment. In the case of USUV, the 24 h pre-treatment and the post-treatment resulted to be equally effective for both compounds, confirming that **ZDL-115** and **ZDL-116** need a time window longer than 2 h to exploit their antiviral action. Altogether, the results led us to formulate two different hypothesis on the potential molecular target of our compounds. Since **ZDL-115** and **ZDL-116** act both in pre-treatment and in post-treatment when added on cells for at least 24 h, they could target a host factor essential for two different phases of viral replication, which signal require a long time to be modulated or suppressed. Alternatively, a potential multi-targeting action could be possible: the compounds could have two different targets with a consequent inhibition of two different replicative cycle phases. The reported antiviral action in the pre-treatment assay indicates a preventive activity that could be mediated by a modification of the cellular milieu in such way that cell become resistant to the infection. This action could be determined by targeting host factors essential for viral infection such as cellular receptors necessary for virus binding to cell or factors involved in the entry process [50,51]. The inhibition of the post-entry stages, i.e. viral genome transcription, translation and replication and virus assembly, could be instead mediated by targeting a specific viral protein, which inhibition led to the suppression of viral progeny production [52-55]. Considering the current results, these observations remain pure speculation and the demonstration of the mechanism of action on cell culture models will be the object a follow-up paper. Nevertheless, in the present work a preliminary investigation of the potential molecular target/s was performed via *in silico* docking analysis (see section 2.8).

Finally, we combined the two active treatments, performing both long pre-treatment and post infection-treatment on Vero cells infected with ZIKV or USUV. We observed that combined treatment did not improve the EC_{50} values in any tested experimental conditions, suggesting no additive action. If confirmed with future experiments, the mechanism of action of these molecules will represent an attractive feature for the further development of a new antiviral drug that could both prevent and cure ZIKV and USUV diseases. In particular, the preventive action could prove useful in contexts where *Aedes* and *Culex* mosquitos (ZIKV and USUV main vectors, respectively) are endemic and for persons that are particularly at risk of contracting these viral infections and developing a sever disease.

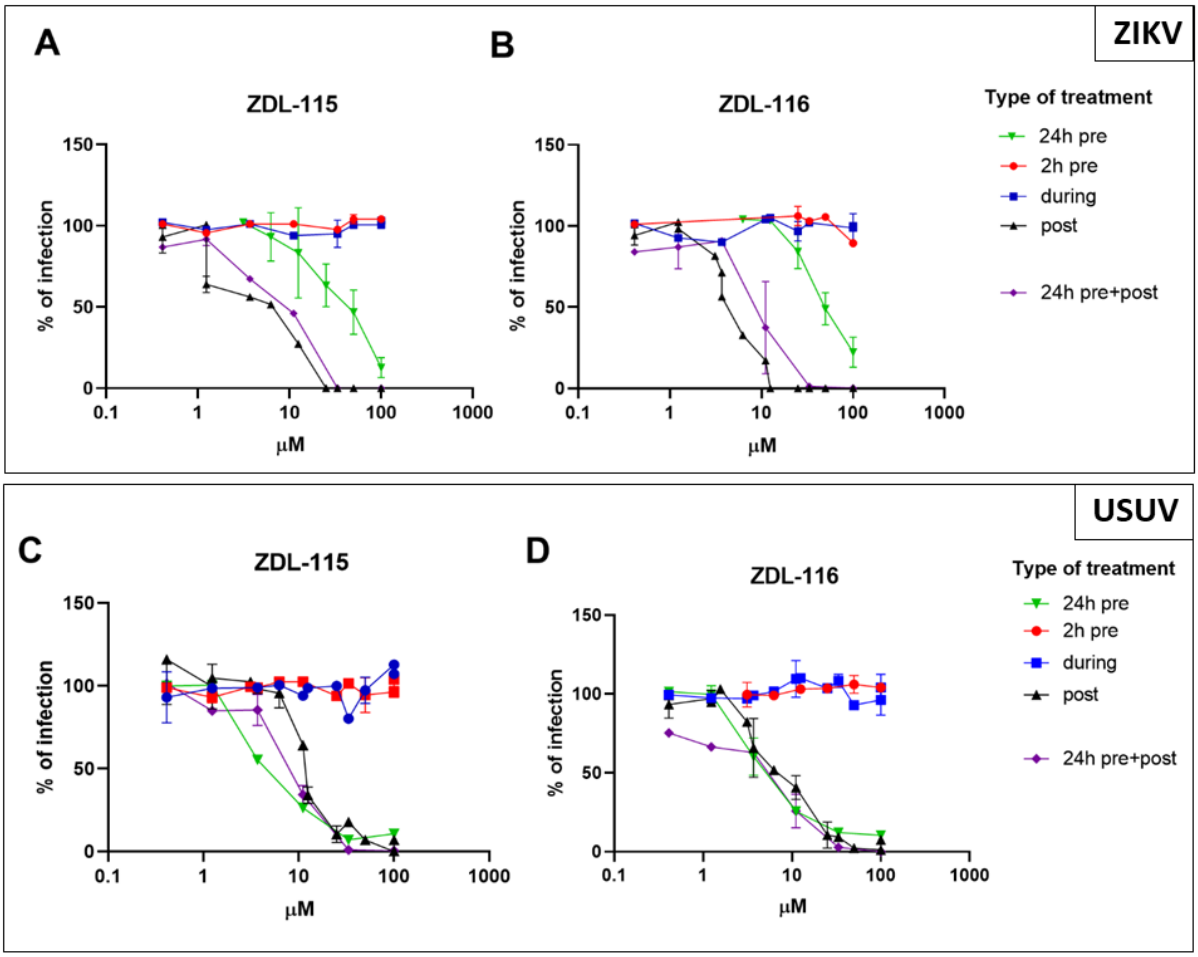

Fig. 5. Time of addition assay. Serial dilutions of **ZDL-115** or **ZDL-116** were added to cells at 24 h or 2 h before infection, during infection, or post-infection. After the incubation time for 24 h (USUV) or 30 h (ZIKV), the ZIKV or USUV-infected cells were fixed with cold acetone-methanol (50:50) and detected by indirect immunostaining. After the identification of the replicative stages inhibited by the compounds, an additional experimental condition was tested by treating cells both before infection for 24 h and post infection in order to evaluate a potential additive activity. (A) **ZDL-115** and ZIKV; (B) **ZDL-116** and ZIKV; (C) ZDL-**115** and USUV; (D) **ZDL-116** and USUV.

2.8. Docking assays for putative binding modes

In order to further investigate the antiviral mechanism of action, a molecular docking study was conducted (**Table 4**, **Fig. 6** and **Figs. S3-S16**). As we previously reported that the scaffold of hexahydropyrrolo[1,2-e]imidazol-1-one can mimic some functions of VD by interacting with VDR and modulating VDR signalling pathway [26,27], we hypothesized that also **ZDL-115** and **ZDL-116** perhaps possess VDR modulatory function. This activity was associated with antiviral action against DENV, ZIKV and JEV [27], but the link between VDR pathways and the replicative cycles of these flaviviruses remains to be elucidated [56]. In

addition, since viral enzymes that are considered important antiviral drug targets, as NS5 RdRp and NS5 MTase, $NS3^{pro}$ and $NS3^{hel}$, interact with nucleosides and nucleotides [18-24], we hypothesized that **ZDL-115** and **ZDL-116** bearing 2-deoxyribose arene could mimic a nucleoside thus targeting the above mentioned viral enzymes. Therefore, some co-crystal complex structures with internal ligand molecules of NS5 RdRp, NS5 MTase, $NS3^{pro}$ and $NS3^{hel}$ were selected for docking study of **ZDL-116**. As ZIKV and DENV share similar viral characteristics [4,57-60] and their viral enzymes have quite resemblance of amino residues at the active sites (**Table 4**), DENV enzymes were also included for docking study. There is currently no reported crystal structures for USUV's proteins. Since WNV and JEV are closely related with USUV [61,62], their available PDB codes were used for representing USUV. Indeed, JEV and WNV exhibit 71% and 68% similarity with USUV and 81% and 75% in proteins, respectively [63,64]. Considering that the 2-deoxy-3β-ribose moiety of **ZDL-116** is closer to natural 2-deoxyribose than 2-deoxy-3-oxo-ribose moiety of **ZDL-115**, we chose to investigate by molecular docking only **ZDL-116**.

Table 4. Molecular docking results of putative binding of **ZDL-116** with potential host and viral targets (receptors) [a]

entry	receptor	Origin/PDB	Amino acids at active sites [b]	Docking score (kcal/mol)			Key interacting amino acid/s
				ZDL116	Internal molecule	Δ [c]	
1	VDR	human/4RUJ [65]		-9.20	-13.35	4.15	R302, W314
2	MTase	ZIKV/5WXB [66]	K61, D146, K182, E218	-6.38	-9.35	2.97	D146, E149, R160
3		DENV2/1I9K [67]	K61, D146, K181, E217	-7.96	-8.06	0.1	R84, W87, K105
4		DENV3/3P97 [68]	K61, D146, K180, E216	-6.41	-9.47	3.06	C82, D146, G148
5		WNV/2OY0 [69]	K61, D146, K182, E218	-6.23	-10.43	4.20	C82, E111, V132
6		ZIKV/5KQR [70]	K61, D146, K181, E218	-4.72	-9.28	4.56	T104, D146, K182
7		JEV/4K6M [71]	K61, D146, K181, E218	-5.58	-9.41	3.83	D146, S150
8	MTase-capping	DENV3/5DTO (full length NS5) [72]	K61, D146, K180, E216	-5.13	-12.18	7.05	T104, E110, D131, E149
9	MTase	ZIKV/5TFR (full length NS5) [73]	K61, D146, K182, E218	-5.95	-10.23	4.28	W87

10	RdRp	DENV3/5K5M [74]	R792, W795, H798	-4.70	-8.0	3.30	D664, R729, Y766
11		ZIKV/5U04 [75]	G793, R794, K802	-5.49	-NA	/	Q620, R623, D665
12		WNV/2HCN [76]	G795, W800, H803	-4.95	-NA	/	D536, D668
13		DENV3/5HMY [77]	S791, H800, Q802	-4.49	-9.05	/	D663
14		JEV/4MTP [78]	R797, W800, H803	-4.05	-NA	/	D541, D668, R742
15	$NS3^{hel}$	ZIKV/5JRZ [79]	K200, D291, R462	-6.35	-NA	/	D291, D540
16	$NS3^{pro}$	DENV2/2FP7 [80]	G82, D129, S135	-6.13	-8.2	2.07	H51, S135, Y130, I155
17		ZIKV/5LC0 [81]	G1454, D1631, S1637	-5.39	-7.9	2.51	K1054, S1135, W1130

[a] diagrams of docking analysis are shown in **Fig. 6** and **Figs. S3-S17**

[b] Amino acid residues are numbered according to the sequence from Uniprot

[c] Δ = docking score of **ZDL-116** - docking score of internal molecule.

The key interacting amino acids for each receptor with **ZDL-116** were revealed and listed in **Table 4**. As shown in **Fig. 6** and **Figs. S3-S16**, it is more frequent that **ZDL-116** could act direct interaction with amino acids of the active site by its *O* of nitro, *O* of carbonyl, *O* of hydroxyl, *H* of hydroxyl and positive *N* of protonated pyrrolidine; meanwhile, the two arenes are able to interact with some receptors and *O* of tetrahydrofuran ring possibly interacts with H_2O in the specific receptor. Particularly, the putative interaction of **ZDL-116** with VDR is shown in **Fig. 6A**, in which **ZDL-116** is surrounded by key amino acids of VDR for its binding to VD and its analogues [65], specifically, **ZDL-116** interacts with VDR by hydrogen bond of guanidyl N-*H* of Arg302 with *O* of nitro group, and by π-cation of indole ring of Trp314 with positive *N* of protonated pyrrolidine. As shown in **Fig. 6B**, ZIKV NS5 MTase and **ZDL-116** construct multiply interactions, such as π-cation interaction between charged guanidyl of Lys105 interacts with *N*-attached phenyl, and hydrogen bonds of *O* of nitro group with amide N-*H* of Val132, O-*H* of primary hydroxyl with carbonyl of Gly81, *O*-*H* of secondary hydroxyl with carbonyl of Asp146, *O*-H of secondary hydroxyl with N-*H* of Lys182, positive N-*H* of protonated pyrrolidine with Glu149, and positive *N*-H of protonated pyrrolidine with Arg160. In the modelling interaction of **ZDL-116** with ZIKV $NS3^{pro}$ (**Fig. 6C**), *O* of nitro group has

hydrogen bond with backbone amine of Lys1054 while two hydroxyl groups of ribose interact with Ser1135 and Trp1130, respectively.

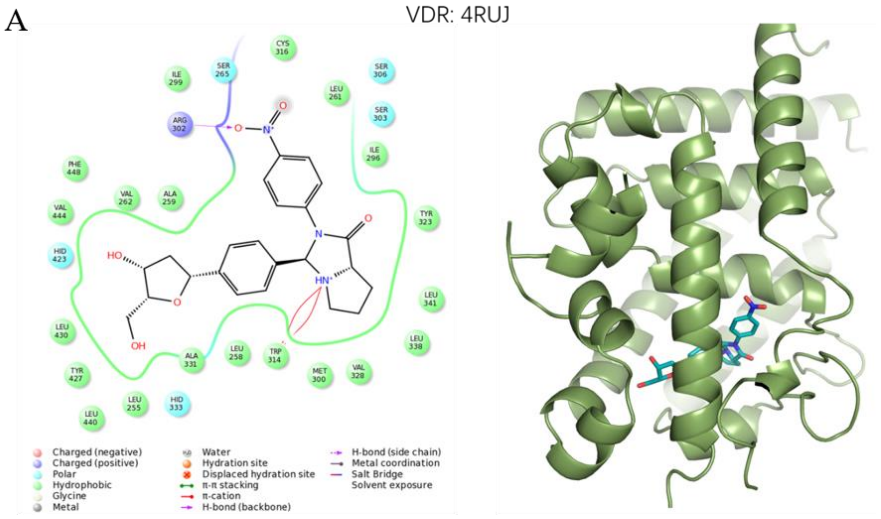

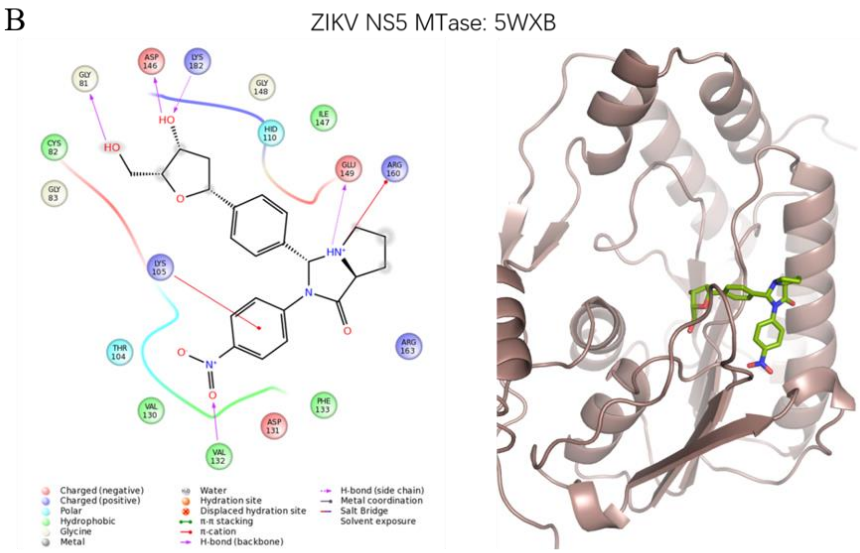

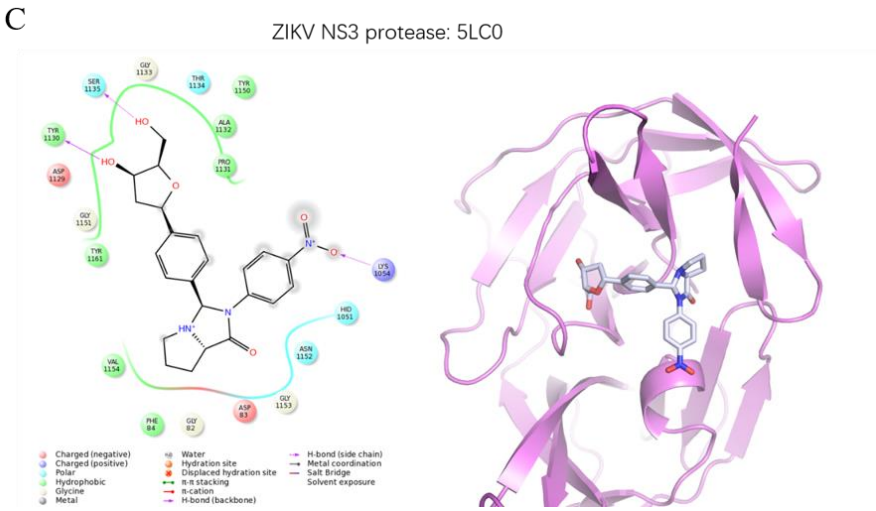

Fig. 6. Docking analysis. (A) Putative interaction of **ZDL-116** with VDR: the details of interaction between **ZDL-116** with VDR (left), and the docked model of **ZDL-116** into VDR pocket (PDB code: 4RUJ [65]) (right). (B) Putative interaction of **ZDL-116** with ZIKV NS5 MTase: the details of interaction between **ZDL-116** with ZIKV NS5 MTase (left), and the docked model of **ZDL-116** into ZIKV NS5 MTase (PDB code: 5WXB [66]) (right). (C) Putative interaction of **ZDL-116** with ZIKV $NS3^{pro}$: the details of interaction between **ZDL-116** with ZIKV $NS3^{pro}$ (left), and the docked model of **ZDL-116** into ZIKV $NS3^{pro}$ (PDB code: 5LC0 [81]) (right)

Two major aspects were considered in our docking analysis: absolute energy release by **ZDL-116**'s binding and relative energy release difference between **ZDL-116** and the internal ligand. The docking results (**Table 4**, entry 1) showed that the binding of **ZDL-116** with human VDR possibly releases -10.15 kcal/mole, which is the highest binding affinity in all potential targets, supporting our proposal of **ZDL-116**'s potential VDR modulating effect. However, the binding difference between **ZDL-116** with the internal molecule is 4.15. Additionally to the results showing **ZDL-116**'s tight interaction with VDR, the docking analysis (**Table 4**) also showed significant docking scores (< -6.0 kcal/mol) for NS5 MTases of DENV2 (**Table 4**, entry 3), DENV3 (**Table 4**, entry 4), ZIKV ((**Table 4**, entry 2 and **Fig. 6B**) and WNV (**Table 4**, entry 5), NS3 helicase of ZIKV (**Table 4**, entry 15) and NS3 protease of DENV2 (**Table 4**, entry 16); while the order of the receptors with the lowest docking score differences (Δ) for the bindings by **ZDL-116** and the internal molecules were DENV2 NS5 MTase (**Table 4**, entry 3), DENV2 $NS3^{pro}$ (**Table 4**, entry 16), ZIKV $NS3^{pro}$ (**Table 4**, entry 17) and ZIKV NS5 MTase (**Table 4**, entry 2). Combining these results, we can speculate that, among these viral enzymes, ZIKV $NS3^{pro}$ and ZIKV NS5 MTase could be the drug target candidates of **ZDL-116** and its analogues. Interestingly, the docking score of **ZDL-116** to DENV2 NS5 MTase is very close to the internal molecule with the marginal difference of 0.1, underlining that NS5 MTase is a potential viral target of **ZDL-116**. The 2^{nd} lowest docking difference by **ZDL-116** and the internal molecule binding to DENV2 $NS3^{pro}$ is in line with our previous work [25], showing that fused bicyclic derivatives of hexahydropyrrolo[1,2-e]imidazol-1-one can interact in particular with DENV2 NS2B-NS3 protease thus inhibiting *in vitro* DENV2 infection.

Overall, these modelling observations suggest that **ZDL-116** possibly act as multi-targeting antiviral agent by activating the host factor/s such as the VDR and also inhibiting viral enzyme/s such as ZIKV MTase and $NS3^{pro}$, thus resulting in the alteration of one or more stages of the viral replicative cycle. Currently the drug target/s of **ZDL-115** and **ZDL-116** is not disclosed yet and we cannot still demonstrate whether or not **ZDL-115** and **ZDL-116** are

multi-targeting antiviral agents. Further study will focus on the experimental elucidation of host and viral targets and on the clarification of the molecular mechanism of action of this series of compounds.

2. Conclusion

In this study, a library of molecules structurally derived from three active scaffolds, the hexahydropyrrolo[1,2-e]imidazol-1-one, the tetrahydroimidazo[1,5-a]quinolin-3(3aH)-one and the tetrahydroimidazo[1,5-a]indol-1-one, has been investigated against ZIKV and USUV infections. Among these compounds, two potent anti-ZIKV and anti-USUV agents, namely **ZDL-115** and **ZDL-116,** with active scaffold bearing 2-deoxyribose moiety were discovered and their preliminary SAR was further explored. By the comparison of them with previously reported anti-flavivirus compound named **ZD-2**, we demonstrated that the introduction of 2-deoxyribose into the scaffold of hexahydropyrrolo[1,2-e]imidazol-1-one increases the solubility and enhances the antiviral activity. The preliminary study of the mechanism of action revealed that either compounds act when added on cells for at least 24 hours, before infection or immediately post-infection, thus suggesting both preventive and therapeutic potential action. The molecular docking *in silico* analysis provided indications of potential molecular targets, showing that **ZDL-116** can tightly bind the host VDR and/or some viral proteins such as ZIKV NS5 MTase and ZIKV $NS3^{pro}$. Further work must still be done to elucidate the molecular mechanism of action and the molecular targets of our compounds and to assess **ZDL-115** and **ZDL-116**'s clinical potential. Nevertheless, our results laid solid foundation for the discovery and the development of a novel anti-flavivirus drug, which would have a significant health impact in a context where there are no fully effective antiviral drugs or vaccines for most flaviviruses and in which a potential next flavivirus epidemic is considered possible.

4. Experimental

4.1. Chemistry

^{1}H and ^{13}C NMR spectra were recorded on a Bruker AV-400 spectrometer at 400 and 100 MHz, respectively, in $CDCl_3$, C_6D_6 and DMSO-d_6 as indicated. Coupling constants (J) are expressed in hertz (Hz). Chemical shifts (δ) of NMR are reported in parts per million (ppm) units relative to the solvent. High

resolution mass spectra (HRMS) data were recorded on Thermo QExactive Focus with Orbitrap analyzer. Unless otherwise noted, materials were obtained from commercial suppliers and used without further purification. Melting points were measured using an YRT-3 melting point apparatus (Shanghai, China) and were uncorrected. HPLC analysis of the purities of **ZDL-115** and **ZDL-116** as following: Waters XBridge C18 (4.6*250mm, 5μm); eluent rate = 1.0 mL/min; T = 25 °C; CH_3CN/H_2O = 70/30, detection wave: 210 nm.

4.2. Synthesis of titled compounds

4-((2*R*,5*R*)-4-(*t*-butyldiphenylsilyloxy)-5-(hydroxymethyl)-2,5-dihydrofuran-2-yl)benzaldehyde (**3**)

2.0 g (5.64 mmol) of compound **1** [33], 1.31 g (5.64 mmol) of *p*-iodobenzenealdehyde (**2**), 258 mg (0.28 mmol) of tris(dibenzylideneacetone)dipalladium ($Pd_2(dba)_3$) and 378 mg (1.24 mmol) of tris(*o*-methylphenyl)phosphine ($(o\text{-tolyl})_3P$) were dissolved in 20 mL of dioxane under nitrogen atmosphere. The mixture was stirred at room temperature (rt) for 10 min before 1.20 mL (8.46 mmol) of triethylamine (TEA) was added. The reaction progress was monitored by thin layer chromatography (TLC) and the reaction was complete after the mixture was stirred at 80 °C for about 6 h. The reaction mixture was diluted by ethyl acetate (EA) and washed with sat. $NaHCO_3$ solution and brine. After the organic phase was dried over anhydrous Na_2SO_4, filtered and then removed volatile solvents to dryness. Silica gel column chromatography gave 1.4 g (55.0% yield) of **3**: colorless oily liquid; ^{1}H NMR (400 MHz, DMSO-d_6) δ 9.94 (s, 1H), 7.78 – 7.69 (m, 6H), 7.52 – 7.39 (m, 8H), 5.55 (m, 1H), 4.93 (t, J = 5.2 Hz, 1H), 4.68 (m, 1H), 4.26 – 4.14 (m, 1H), 3.81 (m, 1H), 3.64 (m, 1H), 1.01 (s, 9H); ^{13}C NMR (101 MHz, DMSO-d_6) δ 193.27, 151.28, 149.88, 136.05, 135.77 (2C), 135.44 (2C), 131.52, 131.16, 130.89, 130.81, 129.75 (2C), 128.60 (2C), 128.36 (2C), 128.16 (2C), 103.16, 84.32, 83.65, 63.03, 26.66 (3C), 19.23; HRMS (ESI) *m/z* found 481.1808$[M+Na]^+$, calculated for $C_{28}H_{30}O_4NaSi$, 481.1806.

(3*R*,7a*S*)-3-(4-((2*S*,5*R*)-4-(*t*-butyldiphenylsilyloxy)-5-(hydroxymethyl)-2,5-dihydrofuran-2-yl)phenyl)-2-(4-nitrophenyl)-hexahydropyrrolo[1,2-e]imidazol-1-one (**7**)

To the solution of 400 mg (1.21 mmol) of compound **6** [25] (trifluoroacetate salt) and 555 mg (1.21 mmol) of **3** in 15 mL of toluene, 0.34 mL (2.42 mmol) of TEA was added. The reaction mixture was refluxed at 110 °C for about 4 h when TLC indicated that the reaction was complete. Distilled off volatile solvents and the residue was treated with EA and then washed with sat. $NaHCO_3$ solution and brine. The organic phase was dried over anhydrous Na_2SO_4 before filtered and evaporated to dryness by Rotovaopor. The residue was purified by silica gel chromatography to afforded 605 mg (74% yield) of **7**: white solid; m. p. 90.6-92.8 °C; ^{1}H NMR (400 MHz, DMSO-d_6) δ 8.23 – 8.15 (m, 2H), 7.85 (d, J = 9.3 Hz, 2H), 7.70 (m, 4H), 7.51 – 7.36 (m, 6H), 7.16 (m, 4H), 6.21 (s, 1H), 5.44 – 5.31 (m, 1H), 4.80 (t, J = 5.3 Hz, 1H), 4.59 (m, 1H), 4.12 (m, 1H), 3.95 (m, 1H), 3.74 (m, 1H), 3.56 (m, 1H), 3.25 (m, 1H), 2.84 (m, 1H), 2.15 – 1.93 (m, 2H), 1.85 – 1.63 (m, 2H), 1.00 (s, 9H); ^{13}C NMR (101 MHz, DMSO-d_6) δ 175.97, 151.15, 143.72, 143.41, 143.19, 139.14, 135.75 (2C), 135.43 (2C), 131.57, 131.26, 130.85, 130.74, 128.56 (2C), 128.37 (2C), 128.15 (2C),

126.35 (2C), 125.12 (2C), 120.61 (2C), 103.32, 84.10, 83.80, 81.75, 64.14, 63.21, 55.57, 27.73, 26.67 (3C), 24.79, 19.22; HRMS (ESI) *m/z* found 698.2659 $[M+Na]^+$, calculated for $C_{39}H_{41}O_6N_3NaSi$, 698.2657.

(3*R*,7a*S*)-3-(4-((2*S*,5*R*)-5-(hydroxymethyl)-4-oxo-tetrahydrofuran-2-yl)phenyl)-2-(4-nitrophenyl)-hexahydropyrrolo[1,2-e]imidazol-1-one (**ZDL-115**)

450 mg (0.66 mmol) of Compound **7** was dissolved in 10 mL of anhydrous tetrahydrofuran (THF) in ice-water bath before 0.80 mL (0.80 mmol) of 1.0 M TBAF in THF solution was added dropwise. The reaction was moved to rt and stirred at rt for about 1 h to finish the reaction when the reaction was complete by TLC monitoring. The reaction mixture was diluted with EA and then treated with sat. $NaHCO_3$ solution and brine, the organic phase was dried over anhydrous Na_2SO_4 before filtered and volatile solvents was removed by Rotavapor. The residue was silica gel chromatographed to provide 220 mg (76% yield) of **ZDL-115**: white solid; m. p. 72.4-73.9 ℃; $[\alpha]^{25}_D$ = +36.82° (*c* 1.168, $CHCl_3$); HPLC purity > 99.54%; ^{1}H NMR (400 MHz, DMSO-d_6) δ 8.21 (d, *J* = 9.3 Hz, 2H), 7.88 (d, *J* = 9.2 Hz, 2H), 7.47 (d, *J* = 8.0 Hz, 2H), 7.33 (d, *J* = 8.0 Hz, 2H), 6.28 (s, 1H), 5.14 (m, 1H), 4.94 (t, *J* = 5.6 Hz, 1H), 4.07 – 3.90 (m, 2H), 3.63 (m, 2H), 3.27 (m, 1H), 2.92 – 2.77 (m, 2H), 2.30 (m, 1H), 2.16 – 1.93 (m, 2H), 1.87 – 1.60 (m, 2H); ^{13}C NMR (101 MHz, DMSO-d_6) δ 214.73, 175.96, 143.73, 143.48, 141.52, 139.46, 127.43 (2C), 126.74 (2C), 125.14 (2C), 120.73 (2C), 83.17, 81.79, 76.62, 64.19, 60.93, 55.59, 45.57, 27.76, 24.80; HRMS (ESI) *m/z* found 460.1480 $[M+Na]^+$, calculated for $C_{23}H_{23}O_6N_3Na$, 460.1479.

(3*R*,7a*S*)-3-(4-((2*S*,4*R*,5*R*)-4-hydroxy-5-(hydroxymethyl)-tetrahydrofuran-2-yl)phenyl)-2-(4-nitrophenyl)-hexahydropyrrolo[1,2-e]imidazol-1-one (**ZDL-116**)

To the ice-water cooled solution of 100 mg (0.23 mmol) of **ZDL-115** in 6 mL THF, 11 mg (0.27 mmol) of $NaBH_4$ was added and the reaction was maintained at 0 ºC for about 1 h until the reaction was complete. The reaction was treated with ice-water and EA, the organic phase was washed with sat. $NaHCO_3$ solution and brine and dried over anhydrous Na_2SO_4 before filtered and distilled to remove solvents. 52 mg (52.0% yield) of **ZDL-116** was afforded after the residue was purified by silica gel chromatography: white solid; m. p. 64.9-66.8 ℃; $[\alpha]^{25}_D$ = -28.395° (*c* 1.134, $CHCl_3$); HPLC purity > 95.94%; ^{1}H NMR (400 MHz, DMSO-d_6) δ 8.24 – 8.15 (m, 2H), 7.92 – 7.83 (m, 2H), 7.36 (d, *J* = 8.0 Hz, 2H), 7.26 (d, *J* = 8.2 Hz, 2H), 6.24 (s, 1H), 4.77 (d, *J* = 4.4 Hz, 1H), 4.69 (t, *J* = 7.6 Hz, 1H), 4.46 (t, *J* = 5.5 Hz, 1H), 4.29 (m, 1H), 3.99 (m, 1H), 3.75 – 3.62 (m, 2H), 3.56 (m, 1H), 3.28 (m, 1H), 2.86 (m, 1H), 2.59 – 2.52 (m, 1H), 2.09 (m, 1H), 1.99 (m, 1H), 1.85 – 1.76 (m, 1H), 1.75 – 1.67 (m, 1H), 1.64 – 1.57 (m, 1H); ^{1}H NMR (400 MHz, DMSO-d_6 + D_2O) δ 8.24 – 8.15 (m, 2H), 7.92 – 7.83 (m, 2H), 7.36 (d, *J* = 8.0 Hz, 2H), 7.26 (d, *J* = 8.2 Hz, 2H), 6.24 (s, 1H), 4.77 (d, *J* = 4.4 Hz, 1H, reduced to very low), 4.69 (t, *J* = 7.6 Hz, 1H), 4.46 (t, *J* = 5.5 Hz, 1H, reduced to very low), 4.29 (m, 1H), 3.99 (m, 1H), 3.75 – 3.62 (m, 2H), 3.56 (m, 1H), 3.28 (m, 1H), 2.86 (m, 1H), 2.59 – 2.52 (m, 1H), 2.09 (m, 1H), 1.99 (m, 1H), 1.85 – 1.76 (m, 1H), 1.75 – 1.67 (m, 1H), 1.64 – 1.57 (m, 1H); ^{13}C NMR (101 MHz, DMSO-d_6) δ 175.98, 143.93, 143.75, 143.45, 138.47, 127.24 (2C), 126.45 (2C), 125.11 (2C), 120.73 (2C), 84.20, 81.91, 78.49, 71.35, 64.18, 60.66, 55.58, 44.11, 27.73, 24.79; HRMS (ESI) *m/z* found 462.1636$[M+Na]^+$, calculated for $C_{23}H_{25}O_6N_3Na$, 462.1635.

(3*R*,7a*S*)-2-(4-aminophenyl)-3-(4-((2*R*,5*R*)-5-(hydroxymethyl)-4-oxo-tetrahydrofuran-2-yl)phenyl)-hexahydropyrrolo[1,2-e]imidazol-1-one (**8**)

Degassed solution of 60 mg (0.14 mmol) **ZDL-115** in 5 mL of THF was treated with 16 mg (0.007 mmol) of 5% Pd/C and hydrogen balloon for 3 h until **ZDL-115** was disappeared. The reaction mixture was filtered through a pad of Celite and washed with EA. After the volatile solvents were evaporated in vaccum, the residue was purified by silica gel chromatography to give about 30 mg (54% yield) of **8**: white solid; m. p. 131.2-132.9 °C; ^{1}H NMR (400 MHz, DMSO-d_6) δ 8.14 (d, J = 9.0 Hz, 1H), 8.07 (d, J = 9.0 Hz, 1H), 7.85 – 7.79 (m, 1H), 7.75 (d, J = 9.1 Hz, 1H), 7.46 (d, J = 7.9 Hz, 2H), 7.33 (d, J = 8.1 Hz, 2H), 6.20 (d, J = 10.7 Hz, 1H), 5.12 (m, 1H), 4.93 (t, J = 5.5 Hz, 1H), 3.99 (m, 1H), 3.95 (m, 1H), 3.62 (m, 3H), 3.27 (m, 2H), 2.90 (m, 1H), 2.79 (m, 1H), 2.37 – 2.24 (m, 1H), 2.13 – 2.05 (m, 1H), 2.04 – 1.95 (m, 1H), 1.87 – 1.76 (m, 1H), 1.75 – 1.64 (m, 1H); ^{13}C NMR (101 MHz, Chloroform-d) δ 213.62, 174.25, 144.29, 140.33, 128.28, 126.83 (2C), 126.79 (2C), 123.86 (2C), 123.18, 115.38 (2C), 84.21, 82.32, 64.45, 61.53, 56.24, 45.31, 29.72, 27.72, 24.89; HRMS (ESI) *m/z* found 430.1739 $[M+Na]^+$, calculated for $C_{23}H_{25}O_4N_3Na$, 430.1737.

(3*R*,7a*S*)-3-(4-(2-hydroxypropan-2-yl)phenyl)-2-(4-nitrophenyl)-hexahydropyrrolo[1,2-e]imidazol-1-one (**10**)

250 mg (0.92 mmol) of compound **6** (hydrochloride salt) and 181.3 mg (1.10 mmol) of aldehyde **9** were dissolved in 10 mL acetonitrile and then treated with 0.2 mL (1.44 mmol) of TEA. The reaction was stirred at 70 °C for about 2 h until the reaction was complete. Diluted with EA and washed with sat. $NaHCO_3$ and brine, the organic phase was dried over anhydrous Na_2SO_4. After filtered and evaporated to dryness, the residue was silica gel chromatographed to yield 234.5 mg (66.8% yield) of compound **10**: white solid; m. p. 118-121 °C; ^{1}H NMR (400 MHz, DMSO-d_6) δ 8.21 (d, J = 9.3 Hz, 2H), 7.89 (d, J = 9.3 Hz, 2H), 7.42 (d, J = 8.1 Hz, 2H), 7.23 (d, J = 8.0 Hz, 2H), 6.25 (s, 1H), 4.98 (s, 1H), 3.97 (dd, J = 9.2, 4.2 Hz, 1H), 3.35-3.29 (m, 1H), 2.88-2.81 (m, 1H), 2.14-2.05 (m, 1H), 2.03-1.95 (m,1H), 1.85-1.76 (m, 1H), 1.73-1.63 (m,1H), 1.36 (d, J = 2.6 Hz, 6H); ^{13}C NMR (101 MHz, DMSO-d_6) δ 175.66, 150.63, 143.40, 142.93, 136.80, 125.64 (2C), 124.97 (2C), 124.71 (2C), 120.06 (2C), 81.28, 70.51, 63.64, 55.08, 31.83 (2C), 27.19, 24.36; HRMS (ESI) *m*/*z* found 382.1759 $[M+H]^+$, calculated for $C_{21}H_{24}N_3O_4$ 382.1767.

(*S*)-1-(*t*-Butoxycarbonyl)-N'-(4-nitrophenyl)pyrrolidine-2-carbohydrazide (**12**)

600 mg (2.79 mmol) Boc-*L*-Pro (**4**) was dissolved in 15 mL dry dichloromethane (DCM) and then cooled to 0 °C before 0.78 mL (9.76 mmol) of 1-methylimidazole was added and stirred for 5 min followed by the addition of 0.26 mL (3.34 mmol) of methanesulfonyl chloride (MsCl). After the reaction mixture was stirred at 0 °C for additional 30 min, 476 mg (2.51 mmol) of *p*-nitrophenylhydrazine (**11**) was added and then moved to rt for 6 h to finish the condensation reaction. After the reaction was treated with EA and washed with sat. $NaHCO_3$ solution and brine, the organic phase was dried over anhydrous Na_2SO_4 and then filtered and distilled volatile solvents. The residue was silica gel chromatographed to afford 780 mg (80% yield) of Boc-protected intermediate of **12**: light yellow solid; m. p. 80.4-82.1 °C; ^{1}H NMR (400 MHz, DMSO-d_6) δ 10.14 (s, 1H), 9.11 (d, J = 19.4 Hz, 1H), 8.05 (m, 2H), 6.78 (m, 2H), 4.22 – 4.14 (m, 1H), 3.41

(m, 1H), 3.32 (s, 1H), 2.30 – 2.14 (m, 1H), 1.94 – 1.75 (m, 3H), 1.43 (d, *J* = 6.1 Hz, 9H); HRMS (ESI) *m/z* found 373.1481 $[M+Na]^+$, calculated for $C_{16}H_{22}O_5N_4Na$, 373.1482.

(3*R*,7a*S*)-3-(4-((2*R*,5*R*)-4-(*t*-butyldiphenylsilyloxy)-5-(hydroxymethyl)-2,5-dihydrofuran-2-yl)phenyl)-2-(4-nitrophenylamino)-hexahydropyrrolo[1,2-e]imidazol-1-one (**13**)

The solution of 600 mg (1.71 mmol) of Boc-protected intermediate of **12** in 8 mL DCM was treated with 2 mL of TFA at rt and stirred for 2 h after the reaction was complete. The volatile solvents was removed and dried under vacuum for 3 h to afford trifluoacetate salt.

The above trifluoacetate salt product was dissolved in 15 mL of toluene and then 690 mg (1.71 mmol) of **3** (ZCR-32) and 0.60 mL (4.28 mmol) of TEA were added in order. The reaction mixture was refluxed for about 6 h until compound **3** disappeared. The volatile solvents were distilled off and the residue was dissolved with EA and washed with sat. $NaHCO_3$ solution and brine. Silica gel chromatography of the crude product produced 605 mg (65% yield) of **13**: light yellow solid; m. p. 108.4-109.6 ℃; ^{1}H NMR (400 MHz, DMSO-d_6) δ 9.10 (s, 1H), 8.06 (m, 2H), 7.77 – 7.60 (m, 4H), 7.54 – 7.37 (m, 6H), 7.20 (d, *J* = 8.6 Hz, 4H), 6.69 (m, 2H), 5.45 (m, 1H), 5.27 (s, 1H), 4.83 (t, *J* = 5.3 Hz, 1H), 4.62 (m, 1H), 4.15 (s, 1H), 3.98 (m, 1H), 3.78 (m, 1H), 3.62 – 3.50 (m, 1H), 3.08 (m, 2H), 2.11 (m, 1H), 1.90 (m, 3H), 1.01 (s, 9H); ^{13}C NMR (101 MHz, DMSO-d_6) δ 172.96, 153.50, 151.22, 143.42, 139.45, 139.26, 135.75 (2C), 135.46 (2C), 131.59, 131.30, 130.89, 130.83, 128.59 (2C), 128.42 (2C), 127.91 (2C), 127.42 (2C), 126.34 (2C), 111.49 (2C), 103.29, 84.13, 83.91, 63.47, 60.24, 28.69, 26.70 (3C), 25.28, 21.24, 19.25, 14.56; HRMS (ESI) *m/z* found 713.2765 $[M+Na]^+$, calculated for $C_{39}H_{42}O_6N_4NaSi$, 713.2766.

(3*R*,7a*S*)-3-(4-((2*R*,5*R*)-5-(hydroxymethyl)-4-oxo-tetrahydrofuran-2-yl)phenyl)-2-(4-nitrophenylamino)-hexahydropyrrolo[1,2-e]imidazol-1-one (**14**)

550 mg (0.80 mmol) of TBDPS-protected product **13** was dissolved in 10 mL of anhydrous THF in ice-water bath and then 0.96 mL (0.96 mmol) of 1 M TBAF solution in THF was added dropwise. After the addition, the reaction was gradually warmed to rt and stirred for about 1 h. Diluted with EA and washed with sat. $NaHCO_3$ solution and brine, the organic phase was dried over anhydrous Na_2SO_4. Filtered and evaporated in vaccum to dryness, the residue was purified by silica gel chromatography to afford 270 mg (75%) of **14**: light yellow solid; m. p. 82.7-84.2 ℃; ^{1}H NMR (400 MHz, DMSO-d_6) δ 9.13 (s, 1H), 8.05 (m, 2H), 7.50 (d, *J* = 7.8 Hz, 2H), 7.40 (m, 2H), 6.71 (m, 2H), 5.32 (s, 1H), 5.18 (m, 1H), 4.97 (t, *J* = 5.5 Hz, 1H), 4.06 – 4.01 (m, 1H), 3.99 (t, *J* = 3.2 Hz, 1H), 3.72 – 3.61 (m, 2H), 3.11 (m, 2H), 2.84 (m, 1H), 2.36 – 2.24 (m, 1H), 2.14 (m, 1H), 1.97 – 1.77 (m, 3H); ^{13}C NMR (101 MHz, DMSO-d_6) δ 214.76, 172.93, 153.50, 141.86, 139.63, 139.28, 127.85 (2C), 127.04 (2C), 126.32 (2C), 111.52 (2C), 83.23, 76.73, 62.13, 60.95, 56.00, 55.38, 45.83, 28.76, 25.29; HRMS (ESI) *m/z* found 475.1592 $[M+Na]^+$, calculated for $C_{23}H_{24}O_6N_4Na$, 475.1588.

(3*R*,7a*S*)-3-(4-((2*R*,4*R*,5*R*)-4-hydroxy-5-(hydroxymethyl)-tetrahydrofuran-2-yl)phenyl)-2-(4-nitrophenylamino)-hexahydropyrrolo[1,2-e]imidazol-1-one (**15**)

To the solution of 100 mg (0.22 mmol) of ketone **15** in 6 mL of THF at 0 °C, 13 mg (0.33 mmol) of $NaBH_4$ was added. The reaction was stirred at 0 °C for about 1 h. After treated with ice-water and EA, the organic phase was washed by sat. $NaHCO_3$ solution and brine, and then dried over anhydrous Na_2SO_4.Filtered and distilled off solvents. Silica gel chromatography provided 52 mg (52.0% yield) of **15**: light yellow solid; m.p.70.3-71.9 °C; ^{1}H NMR (400 MHz, DMSO-d_6) δ 9.11 (s, 1H), 8.04 (m, 2H), 7.34 (m, 4H), 6.70 (m, 2H), 5.29 (s, 1H), 5.06 (d, J = 3.9 Hz, 1H), 5.02 – 4.93 (m, 1H), 4.76 (t, J = 5.6 Hz, 1H), 4.18 (m, 1H), 4.02 (m, 1H), 3.78 (m, 1H), 3.44 (m, 2H), 3.17 (m, 1H), 3.04 (m, 1H), 2.16 – 2.04 (m, 2H), 1.93 (m, 2H), 1.78 (m, 2H); ^{13}C NMR (101 MHz, DMSO-d_6) δ 172.96, 153.51, 144.19, 139.24, 138.69, 127.52 (2C), 126.93 (2C), 126.32 (2C), 111.49 (2C), 84.26, 78.62, 71.38, 60.68, 57.98, 56.01, 44.34, 29.49, 28.73, 25.28; HRMS (ESI) *m/z* found 453.1778 $[M-H]^-$, calculated for $C_{23}H_{25}O_6N_4$, 453.1780.

(3*R*,7a*S*)-3-(3-hydroxy-4-methoxyphenyl)-2-(4-nitrophenyl)-hexahydropyrrolo[1,2-e]imidazol-1-one (**20**)

The procedure of synthesis of compound **20** is the same as the preparation of compound **10**. Compound **20**: 53.9% yield; white solid; m. p. 179-180 °C; ^{1}H NMR (400 MHz, DMSO-d_6) δ 9.07 (s, 1H), 8.21 (d, J = 9.3 Hz, 2H), 7.86 (d, J = 9.4 Hz, 2H), 6.84 (d, J = 8.3 Hz, 1H), 6.72 (d, J = 2.2 Hz, 1H), 6.66 (dd, J = 8.3, 2.2 Hz, 1H), 6.11 (s, 1H), 3.93 (dd, J = 9.1, 4.1 Hz, 1H), 3.70 (s, 3H), 3.28 – 3.22 (m, 1H), 2.84 – 2.78 (m, 1H), 2.15 – 2.05 (m, 1H), 2.01 – 1.95 (m, 1H), 1.83 – 1.75 (m, 1H), 1.72 – 1.66 (m, 1H); ^{13}C NMR (101 MHz, DMSO-d_6) δ 175.65, 147.63, 146.73, 143.49, 142.92, 131.74, 124.67 (2C), 120.13 (2C), 116.98, 113.43, 112.06, 81.36, 63.77, 55.58, 55.01, 27.31, 24.38; HRMS (ESI) *m/z* found 370.1401 $[M+H]^+$, calculated for $C_{19}H_{20}N_3O_5$ 370.1403.

(3*R*,7a*S*)-3-(3,4-dihydroxyphenyl)-2-(4-nitrophenyl)-hexahydropyrrolo[1,2-e]imidazol-1-one (**21**)

The procedure of synthesis of compound **21** is the same as the preparation of compound **10**. Compound **21**: 30.6% yield; white solid; m. p. 217-219 °C; ^{1}H NMR (400 MHz, DMSO-d_6) δ 8.98 (s, 2H), 8.21 (d, J = 9.3 Hz, 2H), 7.85 (d, J = 9.4 Hz, 2H), 6.68 – 6.62 (m, 2H), 6.55 (dd, J = 8.1, 2.1 Hz, 1H), 6.05 (s, 1H), 3.93 (dd, J = 9.2, 4.1 Hz, 1H), 3.27 – 3.21 (m, 1H), 2.79 (m, 1H), 2.15 – 2.05 (m, 1H), 2.02 –1.93 (m, 1H), 1.82 – 1.74 (m, 1H), 1.72 – 1.65 (m, 1H); ^{13}C NMR (101 MHz, DMSO-d_6) δ 175.64, 145.43, 145.37, 143.54, 142.86, 130.10, 124.62 (2C), 120.13 (2C), 117.24, 115.55, 113.45, 81.51, 63.74, 54.94, 27.26, 24.34; HRMS (ESI) *m/z* found 356.1240 $[M+H]^+$, calculated for $C_{18}H_{18}N_3O_5$ 356.1246.

(3*R*,7a*S*)-3-(3,4-dimethoxyphenyl)-2-(4-nitrophenyl)-hexahydropyrrolo[1,2-e]imidazol-1-one (**22**)

The procedure of synthesis of compound **22** is the same as the preparation of compound **10**. Compound **22**: 75.6% yield; white solid; m. p. 55-57 °C; ^{1}H NMR (400 MHz, DMSO-d_6) δ 8.20 (d, J = 9.3 Hz, 2H), 7.85 (d, J = 9.4 Hz, 2H), 6.96 (d, J = 2.0 Hz, 1H), 6.85 (d, J = 8.3 Hz, 1H), 6.73 (dd, J = 8.3, 2.0 Hz, 1H), 6.14 (s, 1H), 4.02 (dd, J = 9.1, 4.2 Hz, 1H), 3.72 (s, 3H), 3.69 (s, 3H), 3.31 – 3.22 (m, 1H), 2.83 (m, 1H), 2.15 – 2.05 (m, 1H), 2.03 – 1.95 (m, 1H), 1.84 – 1.76 (m, 1H), 1.75 – 1.62 (m, 1H); ^{13}C NMR (101 MHz, DMSO-d_6) δ 175.49, 148.98, 148.72, 143.39, 142.97, 131.60, 124.61 (2C), 120.37 (2C), 117.96, 111.46, 110.36, 81.56, 63.76, 55.50, 55.44, 55.02, 27.28, 24.31; HRMS (ESI) *m/z* found 384.1550 $[M+H]^+$, calculated for $C_{20}H_{22}N_3O_5$ 384.1559.

(3*R*,7a*S*)-3-(3-hydroxyphenyl)-2-(4-nitrophenyl)-hexahydropyrrolo[1,2-e]imidazol-1-one (**23**)

The procedure of synthesis of compound **23** is the same as the preparation of compound **10**. Compound **23**: 76.9% yield; white solid; m. p. 203-205 ℃; ^{1}H NMR (400 MHz, DMSO-d_6) δ 9.48 (s, 1H), 8.22 (d, J = 9.3 Hz, 2H), 7.87 (d, J = 9.4 Hz, 2H), 7.13 (t, J = 7.7 Hz, 1H), 6.72 (m, 1H), 6.69 – 6.64 (m, 2H), 6.17 (s, 1H), 3.94 (dd, J = 9.1, 4.1 Hz, 1H), 3.30 – 3.26 (m, 1H), 2.84 (m, 1H), 2.15 – 2.06 (m, 1H), 2.02 – 1.94 (m, 1H), 1.83 – 1.75 (m, 1H), 1.73 – 1.64 (m, 1H); ^{13}C NMR (101 MHz, DMSO-d_6) δ 175.72, 157.68, 143.42, 142.95, 140.67, 129.90, 124.71 (2C), 120.01 (2C), 116.76, 115.25, 112.85, 81.44, 63.74, 55.17, 27.29, 24.39; HRMS (ESI) m/z found 340.1289 $[M+H]^+$, calculated for $C_{18}H_{18}N_3O_4$ 340.1297.

(3*R*,7a*S*)-3-(3-hydroxy-4-methoxybenzyl)-2-(4-nitrophenyl)-hexahydropyrrolo[1,2-e]imidazol-1-one (**28**)

The procedure of synthesis of compound **28** is the same as the preparation of compound **10**. Compound **28**: 93.5% yield; white solid; m. p. 201-203 ℃; ^{1}H NMR (400 MHz, DMSO-d_6) δ 8.82 (s, 1H), 8.31 (d, J = 9.2 Hz, 2H), 8.01 (d, J = 9.3 Hz, 2H), 6.77 (d, J = 8.2 Hz, 1H), 6.63 (d, J = 1.8 Hz, 1H), 6.54 – 6.53 (m, 1H), 5.48 – 5.44 (m, 1H), 3.71 (s, 3H), 3.56 (dd, J = 9.1, 3.9 Hz, 1H), 3.15 – 3.08 (m, 1H), 2.83 – 2.69 (m, 2H), 2.62 (dd, J = 16.3, 9.1 Hz, 1H), 2.06 – 1.95 (m, 1H), 1.86 – 1.76 (m, 1H), 1.69 – 1.59 (m, 2H); ^{13}C NMR (101 MHz, DMSO-d_6) δ 175.45, 146.45, 146.10, 143.38, 142.87, 128.71, 124.84 (2C), 120.48 (2C), 120.38, 117.31, 111.89, 81.15, 64.19, 55.57, 55.23, 38.42, 27.23, 24.32; HRMS (ESI) m/z found 384.1553 $[M+H]^+$, calculated for $C_{20}H_{22}N_3O_5$ 384.1559.

(3*R*,7a*S*)-3-(4-hydroxy-3-methoxybenzyl)-2-(4-nitrophenyl)-hexahydropyrrolo[1,2-e]imidazol-1-one (**29**)

The procedure of synthesis of compound **29** is the same as the preparation of compound **10**. Compound **29**: 82.2% yield; pale yellow solid; m. p. 135-137 ℃; ^{1}H NMR (400 MHz, DMSO-d_6) δ 8.81 (s, 1H), 8.31 (d, J = 9.3 Hz, 2H), 8.02 (d, J = 9.3 Hz, 2H), 6.64 – 6.62 (m, 2H), 6.58 – 6.54 (m, 1H), 5.52 (t, J = 4.7 Hz, 1H), 3.67 (s, 3H), 3.47 (dd, J = 9.3, 4.2 Hz, 1H), 3.16 – 3.10 (m, 1H), 2.87 – 2.78 (m, 2H), 2.63 (dd, J = 16.1, 9.1 Hz, 1H), 2.04 – 1.95 (m, 1H), 1.83 – 1.75 (m, 1H), 1.68 – 1.62 (m, 2H); ^{13}C NMR (101 MHz, DMSO-d_6) δ 175.53, 147.16, 145.29, 143.45, 142.86, 126.78, 124.87 (2C), 122.40 (2C), 120.38, 115.24, 113.92, 81.05, 64.24, 55.59, 55.27, 38.63, 27.31, 24.33; HRMS (ESI) m/z found 384.1554 $[M+H]^+$, calculated for $C_{20}H_{22}N_3O_5$ 384.1559.

(3*R*,7a*S*)-3-(3,4-dihydroxybenzyl)-2-(4-nitrophenyl)-hexahydropyrrolo[1,2-e]imidazol-1-one (**30**)

The procedure of synthesis of compound **30** is the same as the preparation of compound **10**. Compound **30**: 76.4% yield; white solid; m. p. 158-160 ℃; ^{1}H NMR (400 MHz, DMSO-d_6) δ 8.74 (s, 2H), 8.31 (d, J = 9.1 Hz, 2H), 8.01 (d, J = 9.2 Hz, 2H), 6.60 – 6.57 (m, 2H), 6.38 – 6.36 (m, 1H), 5.45 – 5.41 (m, 1H), 3.50 (dd, J = 9.2, 4.1 Hz, 1H), 3.14 – 3.08 (m, 1H), 2.79 – 2.68 (m, 2H), 2.62 (dd, J = 16.1, 8.8 Hz, 1H), 2.02 – 1.95 (m, 1H), 1.84 – 1.76 (m, 1H), 1.68 – 1.62 (m, 2H); ^{13}C NMR (101 MHz, DMSO-d_6) δ 175.49, 144.89, 144.00, 143.42, 142.86, 126.85, 124.87 (2C), 120.61, 120.37 (2C), 117.42, 115.30, 81.23, 64.24, 55.28, 38.39, 27.25, 24.31; HRMS (ESI) m/z found 370.1397 $[M+H]^+$, calculated for $C_{19}H_{20}N_3O_5$ 370.1403.

(3*R*,7a*S*)-3-(4-hydroxybenzyl)-2-(4-nitrophenyl)-hexahydropyrrolo[1,2-e]imidazol-1-one (**31**)

The procedure of synthesis of compound **31** is the same as the preparation of compound **10**. Compound **31**: 68.6% yield; white solid; m. p. 169-170 ℃; ^{1}H NMR (400 MHz, DMSO-d_6) δ 9.24 (s, 1H), 8.31 (d, J = 9.3 Hz, 2H), 8.02 (d, J = 9.3 Hz, 2H), 6.94 (d, J = 8.5 Hz, 2H), 6.63 (d, J = 8.5 Hz, 2H), 5.46 (t, J = 4.8 Hz, 1H), 3.48 (dd, J = 9.2, 4.1 Hz, 1H), 3.12 – 3.06 (m, 1H), 2.80 (d, J = 4.8 Hz, 2H), 2.62 (m, 1H), 2.04 – 1.95 (m, 1H), 1.86 – 1.74 (m, 1H), 1.69 – 1.59 (m, 2H); ^{13}C NMR (101 MHz, DMSO-d_6) δ 175.44, 156.09, 143.38, 142.87, 130.85 (2C), 126.14, 124.89 (2C), 120.35 (2C), 114.92 (2C), 81.18, 64.21, 55.26, 38.19, 27.28, 24.30; HRMS (ESI) m/z found 354.1450 $[M+H]^+$, calculated for $C_{19}H_{20}N_3O_4$ 354.1454.

(3*R*,7a*R*)-3-(4-hydroxy-3-methoxyphenyl)-2-(4-nitrophenylamino)-hexahydropyrrolo[1,2-e]imidazol-1-one (**36**)

The procedure of synthesis of compound **36** is the same as the preparation of compound **10**. Compound **36**: 65.7% yield; white solid; m. p. 92.3-94.2 ℃; ^{1}H NMR (400 MHz, DMSO-d_6) δ 9.03 (s, 2H), 8.04 (s, 2H), 6.92 (d, J = 21.5 Hz, 1H), 6.77 – 6.53 (m, 4H), 5.14 (s, 1H), 4.03 (m, 1H), 3.74 (s, 3H), 3.13 (s, 1H), 2.99 (s, 1H), 2.19 – 2.06 (m, 1H), 1.98 – 1.70 (m, 3H); ^{13}C NMR (101 MHz, DMSO-d_6) δ 172.76 (very low), 153.54 (2C), 148.04, 147.41, 139.13, 130.59, 126.31, 126.31, 116.62, 115.50, 111.43 (2C), ~82.0 (disappeared), 62.26, 60.22, 56.05, 28.76, 25.19.

(3*R*,7a*R*)-3-(4-hydroxy-3-methoxyphenyl)-2-(phenylamino)-hexahydropyrrolo[1,2-e]imidazol-1-one (**37**)

The procedure of synthesis of compound **37** is the same as the preparation of compound **10**. Compound **37**: 68.9% yield; white solid; m. p. 69.3-70.8 ℃; ^{1}H NMR (400 MHz, DMSO-d_6) δ 8.98 (s, 1H), 7.83 (s, 1H), 7.17 – 7.08 (m, 2H), 6.85 (d, J = 1.5 Hz, 1H), 6.75 – 6.67 (m, 3H), 6.64 – 6.57 (m, 2H), 5.10 (s, 1H), 3.92 (dd, J = 8.8, 4.7 Hz, 1H), 3.74 (s, 3H), 3.13 (m, 1H), 2.98 (m, 1H), 2.17 – 2.03 (m, 1H), 1.88 (m, 2H), 1.76 (m, 1H); ^{13}C NMR (101 MHz, DMSO-d_6) δ 172.44, 147.54, 147.14, 146.73, 130.91, 128.92 (2C), 119.97, 118.95, 115.03, 112.11 (2C), 111.14, 81.95, 61.84, 55.57, 55.48, 28.33, 24.75.

(3*R*,7a*R*)-3-(furan-2-yl)-2-(4-nitrophenylamino)-hexahydropyrrolo[1,2-e]imidazol-1-one (**38**)

The procedure of synthesis of compound **38** is the same as the preparation of compound **10**. Compound **38**: 67.2% yield; white solid; m. p. 86.2-87.6 ℃; ^{1}H NMR (400 MHz, DMSO-d_6) δ 9.18 (s, 1H), 8.06 (d, J = 8.6 Hz, 2H), 7.66 (s, 1H), 6.71 (s, 2H), 6.47 (d, J = 3.2 Hz, 1H), 6.41 (s, 1H), 5.46 (s, 1H), 3.96 (s, 1H), 3.24 (m, 1H), 3.02 (s, 1H), 2.20 – 2.05 (m, 1H), 1.97 – 1.72 (m, 3H); ^{13}C NMR (101 MHz, DMSO-d_6) δ 171.81 (very weak), 153.23, 151.60, 143.43, 138.86, 125.86 (2C), 110.99 (2C), 110.45, 109.11, 74.48, 61.51, 55.45, 27.78, 24.81.

(3*R*,7a*R*)-3-(furan-2-yl)-2-(phenylamino)-hexahydropyrrolo[1,2-e]imidazol-1-one (**39**)

The procedure of synthesis of compound **39** is the same as the preparation of compound **10**. Compound **39**: 67.4% yield; white solid; m. p. 120.3-121.6 ℃; ^{1}H NMR (400 MHz, DMSO-d_6) δ 7.97 (s, 1H), 7.64 (dd, J = 1.9, 0.9 Hz, 1H), 7.20 – 7.05 (m, 2H), 6.73 (m, 1H), 6.67 – 6.59 (m, 2H), 6.44 (dd, J = 3.3, 0.9 Hz, 1H), 6.40 (dd, J = 3.3, 1.8 Hz, 1H), 5.39 (s, 1H), 3.87 (dd, J = 9.0, 4.3 Hz, 1H), 3.23 (m, 1H), 3.00 (m, 1H), 2.08 (m, 1H), 1.95 – 1.85 (m, 1H), 1.77 (m, 2H); ^{13}C NMR (101 MHz, DMSO-d_6) δ 173.03, 152.32, 147.32, 143.09, 128.92 (2C), 119.11, 112.10 (2C), 110.34, 108.55, 75.61, 61.62, 55.53, 27.81, 24.80.

(3*R*,7a*R*)-3-(3,4-dimethoxybenzyl)-2-(4-nitrophenylamino)-hexahydropyrrolo[1,2-e]imidazol-1-one (**40**)

The procedure of synthesis of compound **40** is the same as the preparation of compound **10**. Compound **40**: 62.3% yield; white solid; m. p. 90.3-91.5 ℃; ^{1}H NMR (400 MHz, DMSO-d_6) δ 9.35 (s, 1H), 8.12 (s, 1H), 8.10 (d, J = 1.8 Hz, 1H), 6.91 (d, J = 1.7 Hz, 1H), 6.87 – 6.78 (m, 4H), 4.51 (m, 1H), 3.71 (s, 6H), 3.02 (s, 1H), 2.90 (d, J = 13.5 Hz, 1H), 2.73 (m, 2H), 2.06 – 1.97 (m, 2H), 1.77 (m, 2H), 1.68 (d, J = 6.8 Hz, 1H); ^{13}C NMR (101 MHz, DMSO-d_6) δ 173.37 (very weak), 153.29, 148.41, 147.55, 138.93, 128.96, 125.96 (2C), 122.02, 113.76, 111.63, 111.26 (2C), 60.98, 55.94, 55.58, 55.47 (2C), 38.52 (disappeared), 27.57, 24.89.

Primary solubility testing of **ZD-2**, **ZDL-115** and **ZDL-116**

The solubility in *i*-propanol or DMSO of each titled compound was made as usual by the dissolving the quantitative compound in the smallest volume of the solvent.

The aqueous solubility was tested by addition of DMSO stock solution into 1 mL deionized water before clear aqueous solution becomes disappeared. As **ZD-2** has the lowest solubility, we set 1.38% (volume/volume) of the final concentration of DMSO in the aqueous solution as compared solvent point. Based on 1.38% DMSO solution in deionized water, 7 μL **ZDL-115** and 7 μL DMSO showed ≥ 0.897 mg/mL of the aqueous solubility of **ZDL-115** while 7 μL **ZDL-116** and 4 μL DMSO presented ≥ 0.947 mg/mL of the aqueous solubility of **ZDL-116**. (Note: Additional volume of DMSO may make more **ZDL-115** and **ZDL-116** be dissolved in 1.38% DMSO aq. solution, therefore, the solubility should be higher than the calculated value and the symbol of "≥" is used.)

compound	Weight (mg)	Volume of DMSO (mL)	Solubility in DMSO (mg/mL) (stock solution)	Added volume (μL) to 1.0 mL deionized water		Solubility (mg/mL)
				stock solution	DMSO	
ZD-2	3.0	0.080	37.5	14	0	0.518
ZDL-115	2.6	0.020	130	7	7	≥ 0.897
ZDL-116	2.4	0.025	96	10	4	≥ 0.947

4.3. Cell lines and viruses

The African green monkey fibroblastic kidney cells (Vero) (ATCC CCL-81), the lung carcinoma epithelial cells (A549) (ATCC CCL-185) and the hepatocyte derived cellular carcinoma cell line (Huh7) (ECACC, Cat num: 01042712) were grown as monolayers in Dulbecco's modified Eagle's medium (DMEM) (Sigma-Aldrich, Saint Louis, USA), supplemented with 10% (v/v) heat inactivated fetal bovine serum (FBS) (Sigma-Aldrich) and a 1% (v/v) antibiotic solution (penicillin–streptomycin, Sigma-Aldrich) at 37˚C in 5% CO_2 atmosphere.

Two strains of infectious Zika viruses (1947 Uganda MR766 and 2013 French Polynesia HPF2013) were generated as previously described [82]. The viruses were then propagated in Vero cells and titrated by plaque assay. All the antiviral assays were performed with ZIKV MR766 strain, unless otherwise stated.

Usutu virus (Strain: 3345 Isolate: Arb276) was isolated and produced by APHA (Animal & Plant Health Agency – GOV. UK) and kindly provided by the European Viral Archive Global (EVAg). It was propagated in Vero cells and titrated by means of the indirect immunoperoxidase staining procedure, by using a primary mouse monoclonal antibody directed to flavivirus protein E (D1-4G2-4-15 (4G2), Novus Biological) and a secondary antibody peroxidase-conjugated AffiniPure F(ab')2 Fragment Goat Anti-Mouse IgG (H+L) (Jackson ImmunoResearch Laboratories Inc., Baltimore, USA).

The antiviral assays against ZIKV and USUV were performed on the indicated cell line using DMEM supplemented with 2% of FBS.

4.4. ZIKV titration by plaque assay

Vero cells, pre-seeded at a density of 6 x 10^3 in 96 well plates, were inoculated with increasing dilutions of virus prepared in fresh DMEM supplemented with 2% of FBS. After 2 h adsorption at 37 °C, the virus inoculum was removed, cells overlaid with DMEM supplemented with 1.2% methylcellulose and incubated at 37 °C for 72 h. Plates were then fixed and colored with 0.1% of crystal violet for 30 min and gently washed with water. The viral titer was estimated as plaque forming units per ml (PFU/ml) by counting the number of plaques at an appropriate dilution.

4.5. Compound preparation for biological assays

The compounds were dissolved in DMSO to a final concentration of 15 mM and stored at -20 °C until use.

4.6. Virus inhibition assays by focus-reduction or plaque-reduction assays

The anti-ZIKV and anti-USUV activity of the compounds and of the analogues set were first determined by means of focus reduction assays. For the first screening experiments involving 163 different molecules, Vero cells were seeded at a density 1,2 x 10^4/well in 96 well plate. The following day, a fixed amount of ZIKV (MR766) or USUV (multiplicity of infection, MOI = 0.02) was pre-treated with 3 serial concentrations (100 µM, 33 µM and 11 µM) of the tested compound for 1 h at 37°C. These mixtures (virus+ dilutions of compound) were then added to cells for 30 h (ZIKV) or 20 h (USUV) at 37 °C. Control samples (100% of infectivity) were prepared by treating cells with culture medium supplemented with equal volumes of DMSO, corresponding to 1% (v/v) to 0.0014% (v/v) in cell media. After this time, necessary for viral replication, the ZIKV or USUV-infected cells were fixed with cold acetone-methanol (50:50) and detected by indirect immunostaining as described above. Virus foci were counted under inverted optical microscope and the % of viral infection was calculated by comparing the treated with the untreated wells. After the selection of the hit compounds and in order to calculate the effective concentrations inhibiting the 50% and the 90% of infection (EC_{50} and EC_{90}), serial dilutions (from 100 to 0.13 µM) of **ZDL-115** and **ZDL-116** (or EB1089 and chloroquine as controls) were tested against ZIKV and USUV under the experimental protocol reported above. Three different cell lines were used: Vero cells, A549 and Huh7, seeded in 96 well plates at a density of 1.2 x 10^4/well, 1.3 x 10^4/well, 1.6 x 10^4/well, respectively.

To confirm the results, a plaque reduction assay was also performed with ZIKV. Briefly, Vero cells were seeded in 24 well/plate at a density of 6 x 10^4 cell/well. The following day, ZIKV (MOI= 0.005) was treated with serial dilutions of **ZDL-115**, **ZDL-116** for 1 h at 37 °C. Pre-treated virus was then added to cells

for 2 h. Virus inoculum was subsequently removed with 2 gentle washes and cells were overlaid with DMEM supplemented with 1.2% methylcellulose for 72 h to allow plaque formation. Plates were then fixed and colored with 0.1% of crystal violet for 30 min andviral plaques were counted to calculate EC_{50} and EC_{90} values.

GraphPAD Prism 8.0 software (San Diego, USA) was used to fit a variable slope-sigmoidal dose-response curve and calculate the EC_{50} and the EC_{90} values.

4.7. Viability assay and cytotoxicity assay

Confluent cells were treated with the compounds under the same experimental conditions as the antiviral assays. Cell viability or cell cytotoxicity were then determined using the Cell Titer 96 Proliferation Assay Kit (Promega, Madison, WI, USA) or the LDH cytotoxicity assay (Promega, USA) according to the manufacturer's instructions [82,83]. Absorbance was measured using a Microplate Reader (Model 680, BIORAD). The percentage of absorbances of the treated cells to the cells incubated with only culture medium was calculated, and the 50% cytotoxic concentrations (CC_{50}) were determined using GraphPAD Prism 8.0 software (San Diego, the USA).

4.8. Virus yield reduction assay

To test the ability of **ZDL-115** and **ZDL-116** to inhibit multiple cycles of virus replication, Vero cells were seeded at a density of 6.5×10^4 cells/well in 24 well-plates. The day after, cells were treated and infected in duplicate with a mixture of compound (5 µM or 15 µM) and ZIKV or USUV (MOI = 0.1) for 2 h at 37 °C. Following virus adsorption, the virus inoculum was removed by means of three washes and cells were incubated with fresh medium containing the compound (5 µM or 15 µM). Control samples were obtained by infecting cells in the presence of the culture medium and equal volumes of DMSO. Cells were incubated at 37 °C for 48 h, and supernatants and residual cell monolayers were subsequently harvested. They were clarified by low-speed centrifugation and cell-free virus titers were determined by plaque assay (ZIKV) or focus reduction assay (USUV) on Vero cells.

4.9. Time of addition assay

Serial dilutions of **ZDL-115** or **ZDL-116** (from 100 to 0.13 µM) were added to cells before infection for 24 h or 2 h, during infection for 2 h, or post-infection for 24 h (USUV) or 30 h (ZIKV). A combined treatment treating cells both 24h before infection and 24 h (USUV) and 30 h (ZIKV) post infection was also performed. After the incubation time, the ZIKV or USUV-infected cells were fixed with cold acetone-methanol (50:50) and detected by indirect immunostaining as described above. For each experimental condition, the EC_{50} and the EC_{90} values were calculated using GraphPAD Prism 8.0 software (San Diego, USA). After the identification of the replicative stages inhibited by the compounds, an additional experimental condition was tested by treating cells both before infection for 24 h and post infection. The EC_{50} and the EC_{90} values were determined using GraphPAD Prism 8.0 software (San Diego, the USA) in order to evaluate a potential additive action of the two different treatments.

5.10. Molecular Docking

The published crystal structures were used for modelling of possible binding modes. All crystallographic water molecules were deleted. The crystal structures was prepared for docking using the protein preparation wizard in Maestro (Version 9.9.013, Schrödinger), which assigns bond orders and adds hydrogens and missing atoms. The active site was defined with Receptor Grid Generation model. Glide was used for the protein–ligand docking in SP protocol. Multiple stereoisomers, ionization states and three-dimensional (3D) structures of **ZDL-116** as input to the docking calculation were initially generated by LigPrep using the OPLS_2005 force field. Docked binding modes were ranked using the Docking Score. Docking figure was generated using PyMOL.

5.11. Statistical analysis

All the results are presented as the mean values of three independent experiments. The EC_{50} and EC_{90}values of the inhibition curves were calculated from a regression analysis using GraphPad Prism software, version 8.0 (San Diego, the U.S.A.) by fitting a variable slope-sigmoidal dose-response curve. Statistical analysis was performed using Student's t-test, ANOVA Analysis of variance or the F-test, as reported in the Figure legends.

Declaration of competing interest

The authors declare that they have no known competing financial interests or personal relationships that could have appeared to influence the work reported in this paper.

Data availability

Data will be made available on request.

Acknowledgements

This work was supported by the University of Turin, Italy (grant LEMD_RILO_20_01 to DL) and by EU funding within the MUR PNRR Extended Partnership initiative on Emerging Infectious Diseases (Project no. PE00000007, INF-ACT); Taizhou Science and Technology Supporting Plan (Social development) Project (SSF20210034 to ZL and GCZ), Key Scientific Research Projects of Taizhou Polytechnic College (TZYKYZD-22-2 to ZL).

Appendix A. Supplementary material

Supplementary material to this article can be found online at

References

[1] D.M. Morens, A.S. Fauci, Emerging Pandemic Diseases: How We Got to COVID-19, Cell 182 (2020) 1077-1092. Erratum in: Cell 183(2020) 837.

[2] E. Gould, J. Pettersson, S. Higgs, R. Charrel, X. de Lamballerie, Emerging arboviruses: Why today? One Health 4 (2017) 1–13.

[3] T.C. Pierson, M.S. Diamond, The continued threat of emerging flaviviruses, Nat. Microbiol. 5 (2020) 796-812.

[4] R. Hilgenfeld, S.G. Vasudevan, Dengue and Zika: Control and Antiviral Treatment Strategies, Springer Nature Singapore Pte Ltd. 2018.

[5] P. Pielnaa, M. Al-Saadawe, A. Saro, M.F. Dama, M. Zhou, Y. Huang, J. Huang, Z. Xia, Zika virus-spread, epidemiology, genome, transmission cycle, clinical manifestation, associated challenges, vaccine and antiviral drug development, Virology 543 (2020) 34-42.

[6] A. Agarwal, D. Chaurasia D, The expanding arms of Zika virus: An updated review with recent Indian outbreaks, Rev. Med. Virol. 31 (2021) 1-9.

[7] B. Nikolay, A. Dupressoir, C. Firth, O. Faye, C.S. Boye, M. Diallo, A.A. Sall, Comparative full length genome sequence analysis of Usutu virus isolates from Africa, Virol. J. 10 (2013) 217.

[8] L. Barzon, Ongoing and emerging arbovirus threats in Europe, J. Clin. Virol. 107 (2018) 38-47.

[9] M. Clé, C. Beck, S. Salinas, S. Lecollinet, S. Gutierrez, P. Van de Perre, T. Baldet, V. Foulongne, Y. Simonin, Usutu virus: A new threat? Epidemiol. Infect. 147 (2019) e232.

[10] A. Grottola, M. Marcacci, S. Tagliazucchi, W. Gennari, A. Di Gennaro, M. Orsini, F. Monaco, P. Marchegiano, V. Marini, M. Meacci, F. Rumpianesi, A. Lorusso, M. Pecorari, G. Savini, Usutu virus infections in humans: a retrospective analysis in the municipality of Modena, Italy, Clin. Microbiol. Infect. 23 (2017) 33-37.

[11] M. Pacenti, A. Sinigaglia, T. Martello, M.E. De Rui, E. Franchin, S. Pagni, E. Peta, S. Riccetti, A. Milani, F. Montarsi, G. Capelli, C.G. Doroldi, F. Bigolin, L. Santelli, L. Nardetto, M. Zoccarato, L. Barzon, Clinical and virological findings in patients with Usutu virus infection, northern Italy, 2018, Euro. Surveill. 24 (2019) 1900180.

[12] Y. Simonin, O. Sillam, M.J. Carles, S. Gutierrez, P. Gil, O. Constant, M.F. Martin, G. Girard, P. Van de Perre, S. Salinas, I. Leparc-Goffart, V. Foulongne, Human Usutu Virus Infection with Atypical Neurologic Presentation, Montpellier, France, 2016, Emerg. Infect. Dis. 24 (2018) 875-878.

[13] F. Roesch, A. Fajardo, G. Moratorio, M. Vignuzzi, Usutu Virus: An Arbovirus on the Rise. Viruses 11 (2019) 640.

[14] L.L. García, L. Padilla, J.C. Castano, Inhibitors compounds of the flavivirus replication process, Virol. J. 14 (2017) 95.

[15] A. Munjal, R. Khandia, K. Dhama, S. Sachan, K. Karthik, R. Tiwari, Y.S. Malik, D. Kumar, R.K. Singh, H.M.N. Iqbal, S.K. Joshi, Advances in Developing Therapies to Combat Zika Virus: Current Knowledge and Future Perspectives, Front. Microbiol. 8 (2017) 1469.

[16] W. Song, H. Zhang, Y. Zhang, R. Li, Y. Han, Y. Lin, J. Jiang, Repurposing clinical drugs is a promising strategy to discover drugs against Zika virus infection, Front. Med. 15 (2021) 404-415.

[17] C.Q. Sacramento, G.R. de Melo, C.A. de Freitas, N. Rocha, L.V.B. Hoelz, M. Miranda, N. Fintelman-Rodrigues, A. Marttorelli, A.C. Ferreira, G. Barbosa-Lima, J.L. Abrantes, Y.R. Vieira, M.M. Bastos, E. de Mello Volotão, E.P. Nunes, D.A. Tschoeke, L. Leomil, E.C. Loiola, P. Trindade, S.K. Rehen, F.A. Bozza, P.T. Bozza, N. Boechat, F.L. Thompson, A.M. de Filippis, K. Brüning, T.M. Souza, The clinically approved antiviral drug sofosbuvir inhibits Zika virus replication, Sci. Rep. 7 (2017) 40920.

[18] E. Knyazhanskaya, M.C. Morais, K.H. Choi, Flavivirus enzymes and their inhibitors, Enzymes, 49 (2021) 265-303.

[19] I.J.D.S. Nascimento, P.F.D.S. Santos-Júnior, T.M. Aquino, J.X. Araújo-Júnior, E.F.D. Silva-Júnior, Insights on Dengue and Zika NS5 RNA-dependent RNA polymerase (RdRp) inhibitors, Eur. J. Med. Chem. 224 (2021) 113698.

[20] R. Kumar, S. Mishra, Shreya, S.K. Maurya, Recent advances in the discovery of potent RNA-dependent RNA-polymerase (RdRp) inhibitors targeting viruses, RSC Med. Chem. 23 (2020) 306-320.

[21] J.L. Del Sarto, R.P.F. Rocha, L. Bassit, I.G. Olmo, B. Valiate, C.M. Queiroz-Junior, C. Pedrosa, F.M. Ribeiro, M.Z. Guimarães, S. Rehen, F. Amblard, L. Zhou, B.D. Cox, C. Gavegnano, V.V. Costa, R.F. Schinazi, M.M. Teixeira, 7-Deaza-7-fluoro-2'-C-methyladenosine inhibits Zika virus infection and viral-induced neuroinflammation, Antivir. Res. 180 (2020) 104855.

[22] D. Luo, S.G. Vasudevan, J. Lescar, The flavivirus NS2B–NS3 protease–helicase as a target for antiviral drug development, Antiviral Res. 118 (2015) 148–158.

[23] D.A.F. Nunes, F.R.D.S. Santos, S.T.D. da Fonseca, W.G. de Lima, W.S.D.C. Nizer, J.M.S. Ferreira, J.C. de Magalhaes, NS2B-NS3 protease inhibitors as promising compounds in the development of antivirals against Zika virus: A systematic review, J. Med. Virol. 94 (2022) 442-453.

[24] L. Zhang, D. Zhou, Q. Li, S. Zhu, M. Imran, H. Duan, S. Cao, S. Ke, J. Ye, The Antiviral Effect of Novel Steroidal Derivatives on Flaviviruses, Front. Microbiol. 12 (2021) 727236.

[25] Z. Weng, X. Shao, D. Graf, C. Wang, C.D. Klein, J. Wang, G.-C. Zhou, Identification of fused bicyclic derivatives of pyrrolidine and imidazolidinone as dengue virus-2 NS2B-NS3 protease inhibitors, Eur. J. Med. Chem. 125 (2017) 751-759.

[26] B. Xu, M.-Y. Ding,Z. Weng, Z.-Q. Li, F. Li, X. Sun, Q.-L. Chen, Y.-T. Wang, Y. Wang, G.-C. Zhou, Discovery of Fused Bicyclic Derivatives of 1*H*-Pyrrolo[1,2-*c*]imidazol-1-one as VDR Signaling Regulators, Bioorg. Med. Chem. 27 (2019) 3879–3888.

[27] J. Jaratsittisin, B. Xu, W. Sornjai, Z. Weng, A. Kuadkitkan, F. Li, G.-C. Zhou, D.R. Smith, Activity of vitamin D receptor agonists against dengue virus, Sci. Rep. 10 (2020) 10835.

[28] B. Xu, E.M. Lee, A. Medina, X. Sun, D. Wang, H. Tang, G.-C. Zhou, Inhibition of zika virus infection by fused tricyclic derivatives of 1,2,4,5-tetrahydroimidazo[1,5-*a*]quinolin-3(3*aH*)-one, Bioorg. Chem. 104 (2020) 104205.

[29] W. Qian, J.-X. Xue, J. Xu, F. Li, G.-F. Zhou, F. Wang, R.-H. Luo, J. Liu, Y.-T. Zheng, G.-C. Zhou, Design, synthesis, discovery and SAR of the fused tricyclic derivatives of indoline and imidazolidinone against DENV replication and infection, Bioorg. Chem. 120 (2022) 105639.

[30] T. Lan, L.W. McLaughlin, Synthesis of a dA-dT Base Pair Analogue and Its Effects on DNA-Ligand Binding, Bioorg. Chem. 29 (2001) 198–210.

[31] H. Ozaki, T. Kawai, M. Kuwahara, Synthesis and properties of microenvironment-sensitive oligonucleotides containing a small fluorophore, 3-aminobenzonitrile or 3-aminobenzoic acid, Tetrahedron 73 (2017) 7177-7184.

[32] Z.-X. Wang, L.I. Wiebe, E.D. Clercq, J. Balzarini, E.E. Knaus, Syntheses of 4-[1-(2-deoxy-β-D-ribofuranosyl)]- derivatives of 2-substituted-5-fluoroaniline: “cytosine replacement” analogs of deoxycytidine for evaluation as anticancer and antihuman immunodeficiency virus (anti-HIV) agents, Can. J. Chem. 78 (2000) 1081–1088.

[33] K. Temburnikar, Z. Zhang, K. Seley-Radtke, Modified Synthesis of 3′-OTBDPS-Protected Furanoid Glycal, Nucleosides, Nucleotides and Nucleic Acids, 31 (2012) 319-327.

[34] T. Zhang, Z. Wu, Y. Chen, W. Zhao, Z. Yang, F. Zhang, One-Pot Process for Synthesis of Nalbuphine Hydrochloride and Impurity Control Strategy, Org. Process Res. Dev. 24 (2020) 1707−1717.

[35] D.L. Boger, Modern Organic Chemistry, 1999 TSRI Press, p122.

[36] R.N. Farr, G.D. Daves, Efficient Synthesis of 2′-Deoxy-β-D-furanosyl C-Glycosides. Palladium-Mediated Glycal-Aglycone Coupling and Stereocontrolled β- and α-Face Reductions of 3-Keto-furanosyl Moieties, J. Carbohydr. Chem. 23 (1990) 653-660.

[37] R.N. Farr, D.-I. Kwok, G.D. Daves, 8-Ethenyl-1-hydroxy-4-.beta.-D-ribofuranosylbenzo[d]naphtho[1,2-b]pyran-6-one and 8-ethenyl-1-hydroxy-4-(2'-deoxy-.beta.-D-ribofuranosyl)benzo[d]naphtho[1,2-b]pyran-6-one. Synthetic C-glycosides related to the gilvocarcin, ravidomycin, and chrysomycin antibiotics, J. Org. Chem. 57 (1992) 2093-2100.

[38] Z.-X. Wang, L.I. Wiebe, J. Balzarini, E.D. Clercq, E.E. Knaus, Chiral Synthesis of 4-[1-(2-Deoxy-β-L-ribofuranosyl)] Derivatives of 2-Substituted 5-Fluoroaniline: “Cytosine Replacement” Analogues of Deoxy-β-L-cytidine, J. Org. Chem. 65 (2000) 9214-9219.

[39] I. Vicenti, A. Boccuto, A. Giannini, F. Dragoni, F. Saladini, M. Zazzi, Comparative analysis of different cell systems for Zika virus (ZIKV) propagation and evaluation of anti-ZIKV compounds in vitro, Virus Res. 244 (2018) 64-70.

[40] E. Benzarti, M. Garigliany, In Vitro and In Vivo Models to Study the Zoonotic Mosquito-Borne Usutu Virus, Viruses 12 (2020) 1116.

[41] R. Delvecchio, L.M. Higa, P. Pezzuto, A.L. Valadão, P.P. Garcez, F.L. Monteiro, E.C. Loiola, A.A. Dias, F.J.M. Silva, M.T. Aliota, E.A. Caine, J.E. Osorio, M. Bellio, D.H. O'Connor, S. Rehen, R.S. de

Aguiar, A. Savarino, L. Campanati, A. Tanuri, Chloroquine, an Endocytosis Blocking Agent, Inhibits Zika Virus Infection in Different Cell Models, Viruses 8(2016) 322.

[42] C. Li, X. Zhu, X. Ji, N. Quanquin, Y.-Q. Deng, M. Tian, R. Aliyari, X. Zuo, L. Yuan, S.K. Afridi, X.-F. Li, J.U. Jung, K. Nielsen-Saines, F.X.-F. Qin, C.-F. Qin, Z. Xu, G. Cheng, Chloroquine, a FDA-approved Drug, Prevents Zika Virus Infection and its Associated Congenital Microcephaly in Mice, EBioMedicine 24 (2017)189-194.

[43] S. Zhang, C. Yi, C. Li, F. Zhang, J. Peng, Q. Wang, X. Liu, X. Ye, P. Li, M. Wu, Q. Yan, W Guo, X. Niu, L. Feng, W. Pan, L. Chen, L. Qu, Chloroquine inhibits endosomal viral RNA release and autophagy-dependent viral replication and effectively prevents maternal to fetal transmission of Zika virus, Antiviral Res. 169 (2019) 104547.

[44] M. Persaud, A. Martinez-Lopez, C. Buffone, S.A. Porcelli, F. Diaz-Griffero, Infection by Zika viruses requires the transmembrane protein AXL, endocytosis and low pH, Virology 518 (2018) 301-312.

[45] J.M. Smit, B. Moesker, I. Rodenhuis-Zybert, J. Wilschut, Flavivirus cell entry and membrane fusion, Viruses 3 (2011) 160-171.

[46] S.D. Carro, S. Cherry, Beyond the Surface: Endocytosis of Mosquito-Borne Flaviviruses, Viruses 13 (2020) 13.

[47] J.T. Beaver, N. Lelutiu, R. Habib, I. Skountzou, Evolution of Two Major Zika Virus Lineages: Implications for Pathology, Immune Response, and Vaccine Development, Front. Immunol. 9 (2018)1640.

[48] M. Hao, S. Hou, L. Xue, H. Yuan, L. Zhu, C. Wang, B. Wang, C. Tang, C. Zhang, Further Developments of the Phenyl-Pyrrolyl Pentane Series of Nonsteroidal Vitamin D Receptor Modulators as Anticancer Agents, J. Med. Chem. 61 (2018) 3059–3075.

[49] S. Unten, M. Ishihara, H. Sakagami, Relationship between Differentiation-inducing Activity and Hypercalcemic Activity of Hexafluorotrihydroxyvitamin D3 Derivatives, Anticancer Res. 24 (2004) 683-189.

[50] C.D. Cordero-Rivera, L.A. De Jesús-González, J.F. Osuna-Ramos, S.N. Palacios-Rápalo, C.N. Farfan-Morales, J.M. Reyes-Ruiz, R.M. Del Ángel, The importance of viral and cellular factors on flavivirus entry, Curr. Opin. Virol. 49 (2021) 164-175.

[51] Y. Yu, L. Si, Y. Meng, Flavivirus Entry Inhibitors, Adv. Exp. Med. Biol. 1366 (2022) 171-197.

[52] S.K. Samrat, J. Xu, Z. Li, J. Zhou, H. Li, Antiviral Agents against Flavivirus Protease: Prospect and Future Direction. Pathogens, 11 (2022) 293.

[53] Y. Wang, X. Xie, P.Y. Shi, Flavivirus NS4B protein: Structure, function, and antiviral discovery, Antiviral Res. 207 (2022) 105423.

[54] H. Dong, B. Zhang, P.Y. Shi, Flavivirus methyltransferase: a novel antiviral target, Antiviral Res. 80 (2008) 1-10.

[55] D. Luo, S.G. Vasudevan, J. Lescar, The flavivirus NS2B-NS3 protease-helicase as a target for antiviral drug development, Antiviral Res. 118 (2015) 148-58.

[56] C. Lee, Controversial Effects of Vitamin D and Related Genes on Viral Infections, Pathogenesis, and Treatment Outcomes, Nutrients 12 (2020) 962.

[57] W. Hou, R. Cruz-Cosme, N. Armstrong, L.A. Obwolo, F. Wen, W. Hu, M.-H. Luo, Q. Tang, Molecular cloning and characterization of the genes encoding the proteins of Zika virus, Gene 628 (2017) 117-128.

[58] K. Singh, M.G. Martinez, J. Lin, J. Gregory, T.U. Nguyen, R. Abdelaal, K. Kang, K. Brennand, A. Grünweller, Z. Ouyang, H. Phatnani, M. Kielian, H.G. Wendel, Transcriptional and Translational Dynamics of Zika and Dengue Virus Infection, Viruses 14 (2022) 1418.

[59] S. Sundar, S. Piramanayagam, J. Natarajan, A review on structural genomics approach applied for drug discovery against three vector-borne viral diseases: Dengue, Chikungunya and Zika, Virus Genes 58 (2022) 151-171.

[60] R.G. Huber, X.N. Lim, W.C. Ng, A.Y.L. Sim, H.X. Poh, Y. Shen, S.Y. Lim, K.B. Sundstrom, X. Sun, J.G. Aw, H.K. Too, P.H. Boey, A. Wilm, T. Chawla, M.M. Choy, L. Jiang, P.F. de Sessions, X.J. Loh, S. Alonso, M. Hibberd, N. Nagarajan, E.E. Ooi, P.J. Bond, O.M. Sessions, Y. Wan, Structure mapping of dengue and Zika viruses reveals functional long-range interactions, Nat. Commun. 10 (2019) 1408.

[61] G. Kuno, G.J. Chang, K.R. Tsuchiya, N. Karabatsos, C.b. Cropp, Phylogeny of the genus Flavivirus, J. Virol. 72 (1998) 73–83.

[62] C.H. Calisher, E.A. Gould, Taxonomy of the virus family Flaviviridae, Adv. Virus Res. 59 (2003) 1–19.

[63] T. Bakonyi, E.A. Gould, J. Kolodziejek, H. Weissenböck, N. Nowotny, Complete genome analysis and molecular characterization of Usutu virus that emerged in Austria in 2001: Comparison with the South African strain SAAR-1776 and other flaviviruses, Virology 328 (2004) 301–310.

[64] U. Ashraf, J. Ye, X. Ruan, S. Wan, B. Zhu, S. Cao, Usutu Virus: An Emerging Flavivirus in Europe, Viruses 7 (2015) 219-238.

[65] T. Huet, G. Laverny, F. Ciesielski, F. Molnar, T.G. Ramamoorthy, A.Y. Belorusova, P. Antony, N. Potier, D. Metzger, D. Moras, N. Rochel, A vitamin D receptor selectively activated by gemini analogs reveals ligand dependent and independent effects, Cell Rep. 10 (2015) 516-526.

[66] H. Zhou, F. Wang, H. Wang, C. Chen, T. Zhang, X. Han, D. Wang, C. Chen, C. Wu, W. Xie, Z. Wang, L. Zhang, L. Wang, H. Yang, The conformational changes of Zika virus methyltransferase upon converting SAM to SAH, Oncotarget 8 (2017) 14830-14834.

[67] K. Snoussi, S. Nonin-Lecomte, J.L. Leroy, The RNA i-motif, J. Mol. Biol. 309 (2001)139-153.

[68] S.P. Lim, L.S. Sonntag, C. Noble, S.H. Nilar, R.H. Ng, G. Zou, P. Monaghan, K.Y. Chung, H. Dong, B. Liu, C. Bodenreider, G. Lee, M. Ding, W.L. Chan, G. Wang, Y.L. Jian, A.T. Chao, J. Lescar, Z. Yin, T.R. Vedananda, T.H. Keller, P.Y. Shi, Small molecule inhibitors that selectively block dengue virus methyltransferase, J. Biol. Chem. 286 (2011) 6233-6240.

[69] Y. Zhou, D. Ray, Y. Zhao, H. Dong, S. Ren, Z. Li, Y. Guo, K.A. Bernard, P.Y. Shi, H. Li, Structure and Function of Flavivirus NS5 Methyltransferase, J. Virol. 81 (2007) 3891-3903.

[70] J. Coloma, R. Jain, K.R. Rajashankar, A. Garcia-Sastre, A.K. Aggarwal, Structures of NS5 Methyltransferase from Zika Virus, Cell Rep. 16 (2016) 3097-3102.

[71] G. Lu, P. Gong, Crystal Structure of the full-length Japanese encephalitis virus NS5 reveals a conserved methyltransferase-polymerase interface, PLoS Pathog. 9 (2013) e1003549-e1003549.

[72] Y. Zhao, T.S. Soh, S.P. Lim, K.Y. Chung, K. Swaminathan, S.G. Vasudevan, P.-Y. Shi, J. Lescar, D. Luo, Molecular basis for specific viral RNA recognition and 2'-O-ribose methylation by the dengue virus nonstructural protein 5 (NS5), Proc. Natl. Acad. Sci. USA 112 (2015) 14834-14839.

[73] A.K. Upadhyay, M. Cyr, K. Longenecker, R. Tripathi, C. Sun, D.J. Kempf, Crystal structure of full-length Zika virus NS5 protein reveals a conformation similar to Japanese encephalitis virus NS5, Acta Cryst. F Struct. Biol. Commun. 73 (2017), 116–122.

[74] S.P. Lim, C.G. Noble, C.C. Seh, T.S. Soh, A. El Sahili, G.K. Chan, J. Lescar, R. Arora, T. Benson, S. Nilar, U. Manjunatha, K.F. Wan, H. Dong, X. Xie, P.Y. Shi, F. Yokokawa, Potent Allosteric Dengue Virus NS5 Polymerase Inhibitors: Mechanism of Action and Resistance Profiling, PLoS Pathog 12 (2016) e1005737-e1005737.

[75] A.S. Godoy, G.M. Lima, K.I. Oliveira, N.U. Torres, F.V. Maluf, R.V. Guido, G. Oliva, Crystal structure of Zika virus NS5 RNA-dependent RNA polymerase, Nat Commun 8 (2017) 14764-14764.

[76] H. Malet, M.P. Egloff, B. Selisko, R.E. Butcher, P.J. Wright, M. Roberts, A. Gruez, G. Sulzenbacher, C. Vonrhein, G. Bricogne, J.M. Mackenzie, A.A. Khromykh, A.D. Davidson, B. Canard, Crystal structure of the RNA polymerase domain of the West Nile virus non-structural protein 5, J. Biol. Chem. 282 (2007) 10678-10689.

[77] F. Yokokawa, S. Nilar, C.G. Noble, S.P. Lim, R. Rao, S. Tania, G. Wang, G. Lee, J. Hunziker, R. Karuna, U. Manjunatha, P.Y. Shi, P.W. Smith, Discovery of Potent Non-Nucleoside Inhibitors of Dengue Viral RNA-Dependent RNA Polymerase from a Fragment Hit Using Structure-Based Drug Design, J. Med. Chem. 59 (2016) 3935-3952.

[78] P. Surana, V. Satchidanandam, D.T. Nair, RNA-dependent RNA polymerase of Japanese encephalitis virus binds the initiator nucleotide GTP to form a mechanistically important pre-initiation state, Nucleic Acids Res 42 (2014) 2758-2773.

[79] R. Jain, J. Coloma, A. Garcia-Sastre, A.K. Aggarwal, Structure of the NS3 helicase from Zika virus, Nat. Struct. Mol. Biol. 23 (2016) 752-754.

[80] P. Erbel, N. Schiering, A. D'Arcy, M. Renatus, M. Kroemer, S.P. Lim, Z. Yin, T.H. Keller, S.G. Vasudevan, U. Hommel, Structural basis for the activation of flaviviral NS3 proteases from dengue and West Nile virus, Nat. Struct. Mol. Biol. 13 (2006) 372-373.

[81] J. Lei, G. Hansen, C. Nitsche, C.D. Klein, L. Zhang, R. Hilgenfeld, Crystal structure of Zika virus NS2B-NS3 protease in complex with a boronate inhibitor, Science 353 (2016) 503-505.

[82] R. Francese, A. Civra, M. Donalisio, N. Volpi, F. Capitani, S. Sottemano, P. Tonetto, A. Coscia, G. Maiocco, G.E. Moro, E. Bertino, D. Lembo, Anti-Zika virus and anti-Usutu virus activity of human milk and its components, PLoS Negl. Trop. Dis. 14 (2020) e0008713.

[83] A. Civra, M. Costantino, R. Cavalli, M. Adami, M. Volante, G. Poli, D. Lembo, 27-Hydroxycholesterol inhibits rhinovirus replication in vitro and on human nasal and bronchial histocultures without selecting viral resistant variants, Antiviral Res. 204 (2022) 105368.